land

MDPI

Article

Research on the Factors Influencing the Spatial Quality of High-Density Urban Streets: A Framework Using Deep Learning, Street Scene Images, and Principal Component Analysis

Kerun Li

Faculty of Innovation and Design, City University of Macau, Macau 999078, China; kerunli@cityu.edu.mo

Abstract: Urban space constitutes a complex system, the quality of which directly impacts the quality of life for residents. In high-density cities, factors such as the green coverage in street spaces, color richness, and accessibility of services are crucial elements affecting daily life. Moreover, the application of advanced technologies, such as deep learning combined with street view image analysis, has certain limitations, especially in the context of high-density urban streets. This study focuses on the street space quality within the urban fabric of the Macau Peninsula, exploring the characteristics of the street space quality within the context of high-density urban environments. By leveraging street view imagery and multi-source urban data, this research employs principal component analysis (PCA) and deep-learning techniques to conduct a comprehensive analysis and evaluation of the key indicators of street space quality. Utilizing semantic segmentation and ArcGIS technology, the study quantifies 16 street space quality indicators. The findings reveal significant variations in service-related indicators such as the DLS, ALS, DCE, and MFD, reflecting the uneven distribution of service facilities. The green coverage index and color richness index, along with other service-related indicators, are notably influenced by tourism and commercial activities. Correlation analysis indicates the presence of land-use conflicts between green spaces and service facilities in high-density urban settings. Principal component analysis uncovers the diversity and complexity of the indicators, with cluster analysis categorizing them into four distinct groups, representing different combinations of spatial quality characteristics. This study innovatively provides a quantitative assessment of street space quality, emphasizing the importance of considering multiple key factors to achieve coordinated urban development and enhance spatial quality. The results offer new perspectives and methodologies for the study of street space quality in high-density urban environments.

Keywords: high-density cities; street space quality; semantic segmentation; principal component analysis (PCA); Macau

check for updates

Citation: Li, K. Research on the Factors Influencing the Spatial Quality of High-Density Urban Streets: A Framework Using Deep Learning, Street Scene Images, and Principal Component Analysis. *Land* **2024**, *13*, 1161. https://doi.org/10.3390/land13081161

Academic Editor: Mark Altaweel

Received: 1 July 2024
Revised: 24 July 2024
Accepted: 26 July 2024
Published: 29 July 2024

Copyright: © 2024 by the author. Licensee MDPI, Basel, Switzerland. This article is an open access article distributed under the terms and conditions of the Creative Commons Attribution (CC BY) license (https://creativecommons.org/licenses/by/4.0/).

1. Introduction

As globalization continues to deepen and the process of urbanization accelerates, urban spatial quality has become a key indicator for measuring the level of urban development and the quality of life for residents [1,2]. The complexity of urban spatial systems and their impact on residents' daily lives are becoming increasingly prominent [3], especially in urban areas where high density affects the spatial quality and functionality that in turn impact urban vitality [4], achieving spatial equity and high-quality development has become a global challenge. Urban spaces are intricate systems that integrate a multitude of environmental elements, such as infrastructure, buildings, landscape aesthetics, and both pedestrian and vehicular traffic. Urban streets, as pivotal constituents of urban spaces, facilitate a wide array of public activities and embody the urban fabric and overall urban identity [5]. As urban development has transitioned from a focus on expansion to the enhancement of existing resources [3], there is an escalating demand for an elevated living environment. This shift necessitates increasingly nuanced and human-centered approaches to improving the quality of urban public spaces.

Conventional approaches to urban planning and design, primarily qualitative in nature, are often limited by subjectivity, hindering the achievement of unified standardization. Moreover, they lack the capability to deeply analyze the micro-characteristics of public spaces and the intangible qualities of spatial perception, thereby failing to meet the sophisticated demands of modern urban design [6]. The emergence and progression of new data technologies have significantly overcome the data limitations and susceptibility to random influences inherent in traditional urban analytical methods. These technologies have enhanced the credibility and validity of measurement outcomes, enabling the quantification of immaterial urban elements such as quality and vitality, thereby expanding the horizons for the innovative design of public spaces [7–9].

The recent prevalence of street view data platforms, such as Baidu Street View and Google Street View, has enabled the expedited collection of high-fidelity street imagery [2,10]. These data have been instrumental in studies on street safety [11], the degree of street greening [12–14], and the spatial quality of urban streets [15]. Nonetheless, the utilization of big data and novel technologies presents certain issues, including the complexity of urban metrics and the potential disregard for human-centric perspectives. For instance, an overreliance on satellite imagery from an aerial perspective may not consistently correspond with the lived experiences of citizens, especially in terms of the green space perception [13].

In the field of urban spatial system research, the consideration of numerous indicators is essential for a comprehensive assessment of urban space quality. However, previous studies have often relied on multivariate analysis methods, which not only amplify the complexity of the analysis but also struggle to address the intercorrelations among variables, especially within the context of high-density urban environments where such complexities are particularly pronounced. Therefore, this study is dedicated to identifying key indicators with significant impacts on urban space quality and employs dimensionality reduction techniques to streamline the model while retaining vital information, thereby tackling this research challenge. Against this backdrop, the indicators of street quality have become the central constructs of our research, focusing not only on the weight of each indicator but also delving into their variability and interrelationships.

This study employs deep learning and street view image analysis technologies to construct a high-precision, multidimensional evaluation framework. It aims to extract and quantify key spatial quality indicators from a vast array of street view image data. Utilizing methods such as principal component analysis (PCA), semantic segmentation, and cluster analysis, this study seeks to uncover the critical factors influencing street space quality and their intrinsic connections. Based on this foundation, we pose a central research question: How can multiple key factors be synthesized in the context of high-density urban environments to optimize street space quality, thereby achieving coordinated urban development and enhancement of spatial quality? This question is pivotal for guiding urban planning and design, as well as for improving the quality of life for residents.

2. Literature Review

2.1. Machine Learning and Street View Images

Within the domain of urban studies, the amalgamation of street view imagery and machine learning has presented innovative approaches and tools for examining urban spatial quality [11,12]. Traditional urban research has frequently been hindered by the challenges of data acquisition and processing inefficiency. However, the utilization of street view imagery in conjunction with machine learning has adeptly addressed these challenges [3]. This synergy has alleviated the previous inaccessibility of foundational street data and the inefficient use of street view imagery. The application of pertinent machine-learning algorithms not only provides detailed foundational data for the study of spatial quality but also expedites the processing of extensive datasets while maintaining a high degree of refinement. This resolves the previous issue where large-scale data lacked detail and detailed local data could not encapsulate the broader context, thereby rendering the technical measurement of previously "untestable" spatial qualities viable [3,16].

Street view imagery (SVI) captures the essence of the urban environment by providing an authentic human viewpoint for observing urban landscapes. Its broad coverage and granular spatial sampling have been extensively applied in urban built environment research across various scales [17,18]. The emergence of this extensive dataset has opened up new opportunities for the digitization of the world, enabling researchers to investigate the physical urban environment and human activities on a large scale. SVI acts as a dependable data source for scrutinizing the built environment and its correlation with health outcomes [19]. Scholars have utilized street view imagery to construct three-dimensional urban models for an objective understanding of the relationship between location and the physical environment [20,21], to delineate urban morphology through the mapping of image locations [22], and to analyze the visual components of urban spaces from a perceptual standpoint, encompassing urban greenery [1,2].

In the domain of computer vision, the advent of deep convolutional neural networks (DCNNs) and DCNN-based image content analysis methods has revolutionized numerous fields. DCNNs are hierarchical invariant models for high-dimensional data processing [6], and they have been proven effective in learning features from large-scale datasets [23]. Utilizing urban landscape spatial imagery, applications have spanned the prediction of socioeconomic indicators [24], forecasting emotional responses to images [25], quantifying urban imagery [26], assessing and mapping urban tree cover [27], monitoring community changes [28], predicting the visual quality of urban environments [26], calculating urban naturalness [29], green space [30,31], urban color palettes [32,33], and learning navigation within cities without maps [34].

Image semantic segmentation is a significant topic within the field of computer vision [35]. Research and applications based on semantic segmentation technology in street space encompass a wide range of areas. These include analyzing the distribution of and changes in urban greenery using street view imagery [12,36], exploring the association between the built environment and health outcomes [11,19,37–42], assessing the quality of the urban walking environment through street view imagery [43–50], and evaluating the visual perception of urban environments using street view imagery [47,51]. They also include examining the application of street view imagery in assessing urban accessibility [47,51,52], analyzing the spatial distribution of urban poverty through street view imagery [53–55], assessing the sense of safety in urban environments using street view imagery [47,52], exploring the enclosure of urban street spaces [47], investigating the factors influencing urban crime using street view imagery [56,57], and examining the impact of the urban environment on mental health [5,56,57].

Through semantic segmentation techniques, researchers are capable of automatically identifying and classifying various elements within street view images to generate precise urban landscape data. Such data not only aid in understanding the physical characteristics of urban spaces but also facilitate the analysis of the urban environment's impact on residents' quality of life and health. For instance, studies by Li [1] and Long [2] have demonstrated that the distribution and quality of urban green spaces significantly affect residents' mental health. Furthermore, the integration of street view imagery with machine-learning technologies has provided new tools for urban planning and policy-making. By analyzing visual elements within street view images, researchers can assess the potential impacts of different urban planning proposals and offer optimization suggestions. For example, Middel [58] provided urban planners with vital information regarding the spatial distribution and characteristics of communities in Philadelphia by classifying and analyzing visual features across different neighborhoods.

In summary, the fusion of street view imagery and machine-learning technologies has significantly enriched the dimensions of urban street space research, enhancing both the efficiency and accuracy of studies [2,10] and deepening our comprehension of the physical attributes of urban spaces and residents' lived experiences [6]. This integrated approach offers a solid scientific foundation for urban planning and policy-making. However, the variability and interconnectivity of multiple indicators in urban environmental research

can lead to collinearity among these indicators, especially in the study of complex and high-density cities.

2.2. Street View Image Indicators

Historically, urban environmental research has been underpinned by key theories such as Lynch's [59] theory of the five elements of urban imagery, where streets, as pathways, fundamentally interact with other elements—landmarks, nodes, districts, and edges—to establish the city's overall coherence and significance [60]. Within the built environment discourse, the 5Ds framework introduced by Ewing [60] has seen extensive application, emphasizing dimensions such as the density [61–63], land use diversity [64], street design characteristics [65], destination accessibility [62,66], and transit accessibility [61,67]. The Athens Charter further delineates urban activities into four primary categories: dwelling, transportation, work, and recreation [68]. These theoretical frameworks have substantiated the study of urban street space quality. Urban-planning scholars and geographers have, therefore, investigated the importance of these theories and the essential nature of their foundational elements from diverse perspectives [2,69,70]. The constituents of street space quality are delineated into secondary indicators, including visual permeability, public service facility density, functional diversity, crowd aggregation, commercial facility density, color richness, transit stop count, vehicle interference index, pedestrian walkway proportion, park and green space ratio, sky visibility, and green view rate.

The integration of computer vision in environmental studies has significantly propelled the field forward. Machine-learning algorithms, including SegNet, DeepLab [71], and YOLO [72], are harnessed to identify and quantify key elements supported by current analytical techniques. Street view images are labeled based on urban street elements and subsequently utilized to train semantic segmentation models. Commonly labeled urban elements include roads, vegetation, sky, and buildings, which are quantified into urban landscape indicators such as enclosure, accessibility, greening rate, and green cover rate.

The key spatial features in prior street view image research encompassed the green view rate, sky visibility, building interface, street motorization degree, pedestrian space, human scale, enclosure, complexity, and diversity [3]. The spatial elements were further defined to include the street scale, sky visibility, harmony, walkability, street furniture, green view rate, road motorization, road section morphology, and building interface, with non-operational factors set aside. Six operational spatial feature elements were identified as crucial: street green view rate, sky visibility, building interface, pedestrian space, road motorization degree, and diversity [47]. Middel [58] categorized the visual components into six classes—sky, trees and plants, buildings, impervious surfaces, permeable surfaces, and non-permanent objects—and analyzed their spatial distribution and correlation in Philadelphia. This classification aids in deciphering the composition of urban landscapes and their variance across neighborhoods, offering valuable insights for urban planning and design. Shen [73] conducted street evaluations across four dimensions: spatial form, functional attributes, perceptual character, and behavioral usage, with indicators including walkability, ground floor transparency, pedestrian scale, accessibility for pedestrians, functional density, functional diversity, nighttime lighting, green view rate, and the density of characteristic buildings. Li [74] developed an evaluation index comprising 12 layers of indicators constructed around the dimensions of comfort, safety, convenience, and vitality.

In summary, the current body of research demonstrates that street view imagery, acting as a representative of urban physical appearance, leverages deep-learning techniques to extract scene elements. These elements form the basis for the classification of street metrics across several dimensions, such as the spatial configuration, functional attributes, aesthetic perception, and behavioral utilization [6,18,75]. The assessment also includes prevalent indicators like the density and diversity of points of interest (POIs) [74]. The research in the domain of street view imagery has yielded significant findings. Nonetheless, the selection of street landscape indicators by scholars predominantly relies on subjective choices informed by the prior literature. Therefore, it is imperative to conduct research

that quantitatively analyzes the significance and weight of a comprehensive set of street quality indicators.

2.3. Research Gap

Under the auspices of globalization and urbanization, the quality of urban space has emerged as a pivotal metric for gauging the developmental caliber of cities and the quality of life of their residents [1,2]. This study takes the Macau Peninsula as a case in point; being a region characterized by intense urbanization and a concentration of tourism and commercial activities, the study of its street space quality holds significant practical implications [76]. Consequently, an in-depth examination of the multiple indicators of street space quality on the Macau Peninsula, uncovering their variability and interconnectivity, is of considerable value for the optimization of urban planning and design. This research endeavors to apply principal component analysis and deep-learning techniques to comprehensively analyze and assess key urban streetscape indicators, addressing the dearth of research on high-density cities in the existing literature. This study specifically aims to achieve the following objectives:

(1) To explore the manifestations of various street space quality indicators in high-density cities. The research employs multivariate analysis methods, which, while enhancing the complexity and difficulty of the analysis, also allows for the identification of indicators of significant relevance to the research topic through principal component analysis.
(2) To evaluate the distribution and variability of various street space quality indicators in high-density cities. By calculating the coefficients of variation, the study assesses the stability and consistency of each indicator, offering a reference for policymakers to improve and manage street quality.
(3) To investigate the interrelationships among various street space quality indicators in high-density cities. Correlation analysis will reveal the relationships between different indicators, particularly within the context of high-density urban street space indicators.
(4) To discuss the weighting and cluster analysis of various street space quality indicators in high-density cities. Principal component analysis and cluster analysis will be utilized to identify and categorize clusters of indicators with similar characteristics, thereby shedding light on the diversity and complexity of street space quality in high-density urban areas.

To summarize, this research is not only designed to streamline the assessment process of street space quality in high-density cities but also aspires to provide a scientific basis for urban planning and policy-making by considering multiple key indicators. The ultimate goal is to achieve coordinated urban development and enhance the quality of urban spaces.

3. Materials and Methods

3.1. Research Area

Macau is located on the southeast coast of China, 60 km to the west of Hong Kong. It is composed of four distinct regions: the Macau Peninsula, Taipa, Cotai, and Coloane. The Macau Peninsula is the central area of Macau, with a small section of its northeastern territory connected to mainland China. According to the Statistics and Census Service of the Macau Special Administrative Region (May 2024 data), Macau has a total population of 686,000. This results in a high population density of over 20,000 people per square kilometer, a defining characteristic of the region [76]. The gaming and tourism sectors are the main economic drivers of Macau.

Macau's history as a Portuguese colony for nearly 450 years has imbued the city with a blend of Chinese and Portuguese architectural styles, further diversified by the presence of residents from the Philippines, Portugal, and other countries. This multicultural demographic affects the accessibility of urban green spaces [1,77]. The Macau Peninsula, which houses 84.88% of Macau's total population, is not only the earliest developed area with a history of more than four centuries but is also a designated the World Cultural Heritage site.

Spanning approximately 9.3 square kilometers, the Macau Peninsula consists of five administrative districts: the Parish of Our Lady of Fatima, the Parish of St. Anthony, the Cathedral Parish, the Parish of St. Lawrence, and the Parish of St. Lazarus. Given the study's aim to investigate the quality of street space in high-density urban contexts, the Macau Peninsula has been chosen as the research focus, as shown in Figure 1.

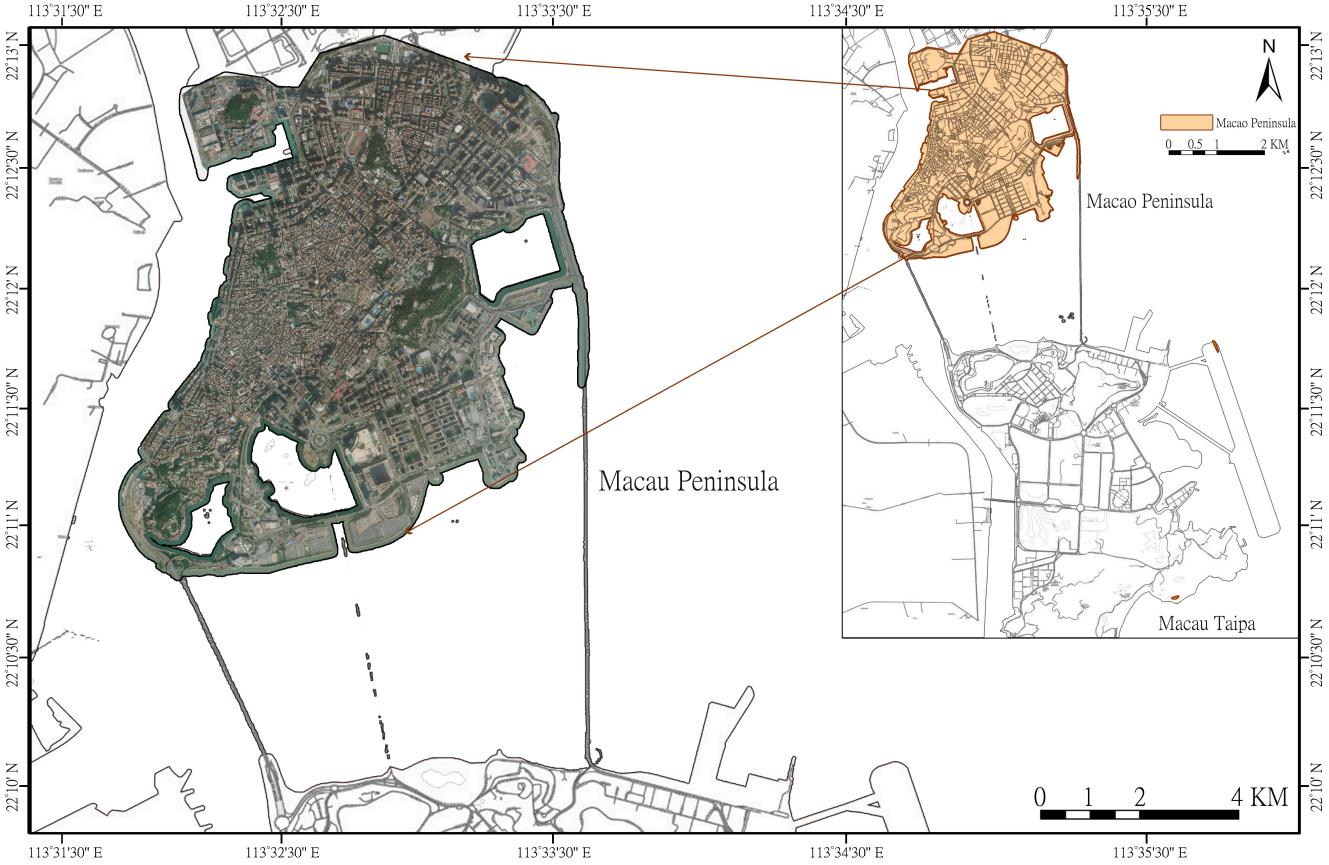


Figure 1. Research area.

This study's framework comprises several stages, including data collection, semantic segmentation, indicator quantification, and result analysis. Data are gathered from a variety of sources, such as Open Street Map road networks, street view imagery, and points of interest (POI) data. Semantic segmentation of the street view images is performed using deep-learning algorithms. This is followed by the development and normalization of indicators, calculation of coefficients of variation, and principal component analysis, as illustrated in Figure 2.

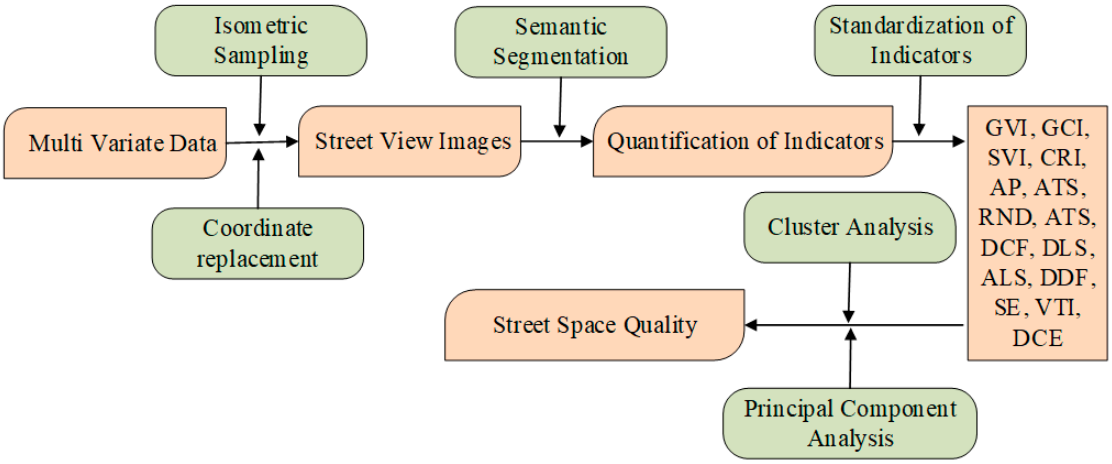


Figure 2. Research framework for street space quality.

3.2. Data Collection

(1) OSM Road Network

The Open Street Map (OSM) road network data were derived from the Open Street Map platform (https://www.openstreetmap.org/ (accessed on 19 June 2024)). Following simplification, topological verification, and intersection segmentation, the study area comprised 2384 distinct road segments. To establish a basis for the street view image collection, the network was enhanced with sampling points at 50 m intervals, as illustrated in Figure 3.

(2) Street View Image

One of the pioneering developments in this field was the launch of Google's Street View program in 2007, which was subsequently complemented by the active participation of Baidu Maps from China, contributing a vast collection of 360-degree panoramic images of roads [49]. The study area was meticulously mapped to identify 2384 roads, and along this network, a street view sampling layer of 12,721 points was created at 50 m intervals. Using the coordinates of these designated points, metadata for the Baidu Street View (BaiduSV) panoramas was obtained via the API interface [75]. The field of view parameter was configured to 360° to capture the entire visual spectrum. A Python script was developed to fetch these panoramic images, thus amassing a collection of 12,721 images in total. Subsequently, mean processing of the collected image data at each sampling point was conducted, culminating in a refined dataset comprising 6667 valid street view images.

(3) POI Data

The POI data were extracted through the Google Maps API, followed by data cleansing, projection transformation, and vectorization using ArcMap for georeferencing and simplification. The categorized POIs were then appended to proximate roads, with a 100 m connection distance, to serve as evaluation units and quantification carriers. These data were reclassified according to their functional roles, and indicators such as the facility convenience dimension were computed.

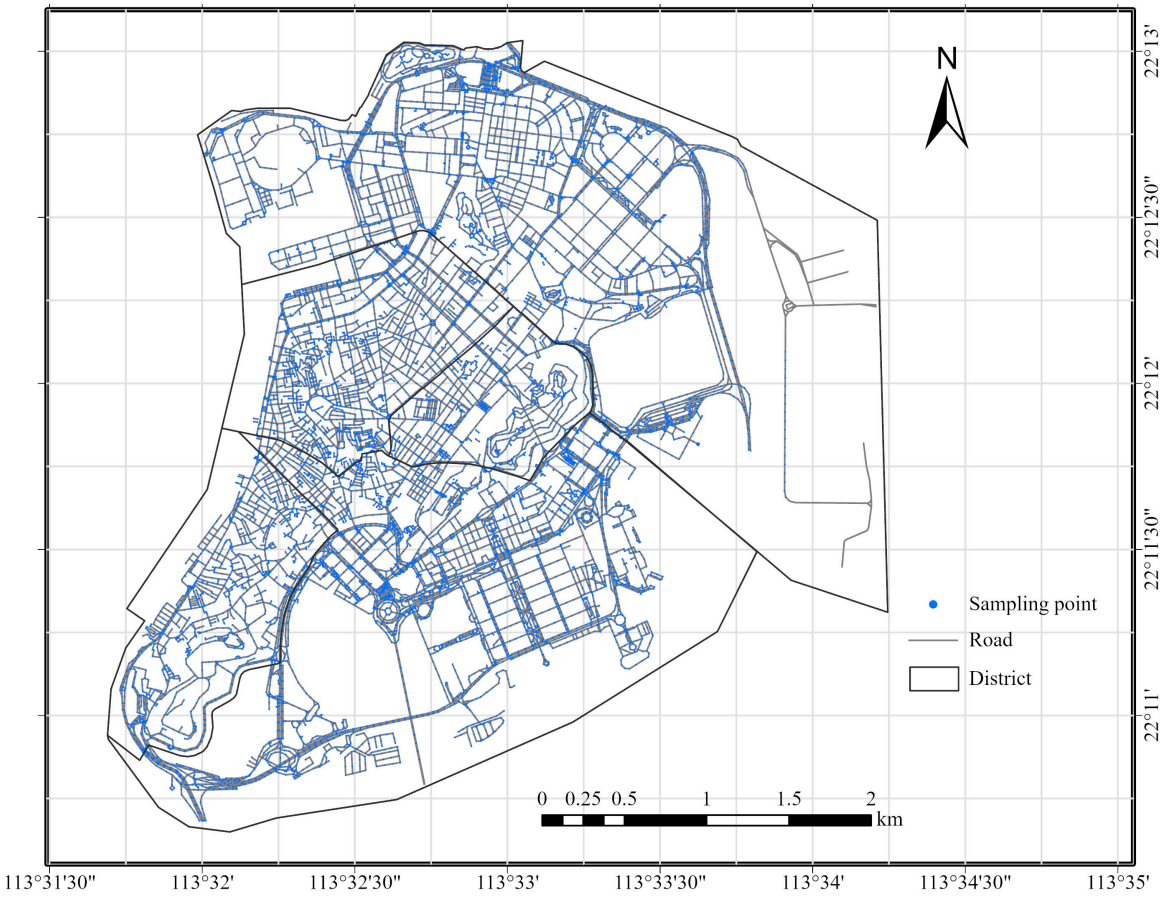


Figure 3. Distribution of collection points based on the road network diagram.

3.3. Sample Dataset and Semantic Segmentation

This study employs deep-learning-based semantic segmentation techniques, specifically the Mask2Former model, which has been trained using the Cityscapes open-source dataset to extract features from street view imagery and to compute the ratios of various feature indicators. The Cityscapes dataset consists of 5000 annotated high-resolution images, distributed as 2975 for training, 500 for validation, and 1525 for testing, each with a resolution of 1024 × 2048 pixels. The dataset's 34 categories enable the extraction of the pixel proportion and location data for 19 distinct urban elements, such as buildings, vegetation, roads, sky, and vehicles. These data are then used to calculate 16 specific indices. The Simpson index is also applied to assess the color diversity of the street spaces.

By leveraging the Cityscapes scene parsing and segmentation database as the training dataset, the Mask2Former model semantically segments the street view images into 151 distinct street objects [18,75,78]. This study processes 50,896 street view images through the FCN-8s model to determine the semantic segmentation outcomes for each object within the images (as depicted in Figure 4). The Mask2Former model, developed by Cheng [79], is highlighted for its ability to efficiently handle diverse image segmentation tasks. It incorporates a masked attention mechanism that localizes features by limiting cross-attention to within the predicted mask areas. This innovative approach not only enhances the research efficiency by a factor of at least three but also surpasses the performance of specialized architectures on four major datasets.

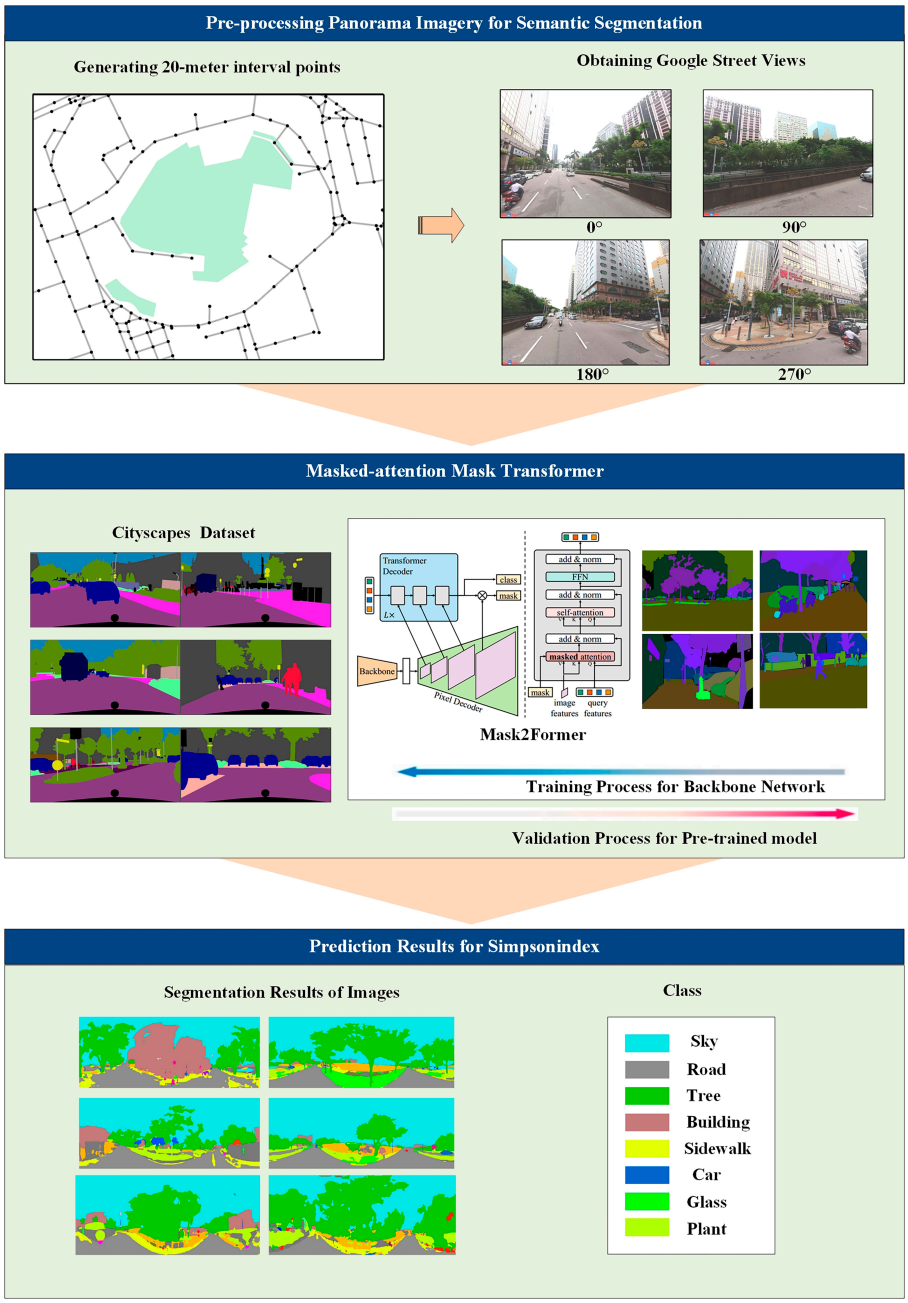


Figure 4. Technical roadmap for semantic segmentation of street view images.

3.4. Construction of Evaluation Indicators System

This research integrates street view data with machine-learning algorithms to evaluate street quality indicators on a large scale. The construction of the evaluation indicator system is informed by the spatial elements proposed by Katz [80] and Montgomery [81], encompassing the street scale, sky visibility, sense of harmony, walkability, street furniture, green view rate, motorization of roads, road section morphology, and building interface. Building upon this foundation, Ewing [47] identified six operational spatial characteristic elements: street green view rate, sky visibility, building interface, pedestrian space, degree of road motorization, and diversity. Ye [76] expanded this framework to include six key spatial features in the analysis of street view images.

Shen [73] contributed a dimensional evaluation of streets, encompassing the spatial form, functional attributes, aesthetic perception, and behavioral usage, with specific indicators such as the walkability, ground floor transparency, pedestrian scale, accessibility

for pedestrians, functional density, functional diversity, nighttime lighting, green view rate, and characteristic building density. Li [74] further developed an evaluation indicators across four dimensions—comfort, safety, convenience, and vitality—resulting in 12 layered indicators.

Synthesizing the aforementioned studies, this research selects key elements measurable with current analytical techniques, excluding non-operational factors. Focusing on the Macau Peninsula, the study employs image semantic segmentation and ArcGIS technology to derive 16 indicators from street view images, road networks, and POI data. These indicators include the green view index (GVI), green coverage index (GCI), sky view index (SVI), color richness index (CRI), accessibility of pavement (AP), accessibility of transportation services (ATS), road network density (RND), accessibility of transportation station (ATS2), diversity of commercial facilities (DCF), density of leisure and shopping (DLS), accessibility of life services (ALS), diversity of diverse functions (DDF), street enclosure (SE), vehicle traffic index (VTI), density of cultural and educational facilities (DCE), and medical facilities density (MFD). Definitions of and data sources for these indicators are detailed in Table 1.

Table 1. Street space quality indicators and their data sources.

NO.	Indicators Layer	Explanation	Data Sources
1	Green View Index, GVI	The average proportion of plant elements in street view images within street units reflects the degree of greening from a humanistic perspective.	Semantic segmentation
2	Green Coverage Index, GCI	The proportion of green coverage area in the total area of the region reflects the overall greening level of the city.	Remote-sensing data
3	Sky View Index, SVI	The average proportion of sky elements in street view images within street units reflects the openness of space.	Semantic segmentation
4	Color Richness Index, CRI	Use Simpson index to calculate the diversity of streetscape elements within street units to reflect spatial richness.	Semantic segmentation
5	Accessibility of Pavement, AP	The average proportion of image sidewalks and pedestrian elements in the street unit reflects the walkable space of the street.	Semantic segmentation
6	Accessibility of Transportation Services, ATS	The POI density of traffic services within a 100 m buffer zone on the road reflects the convenience of traffic services.	POI data
7	Road Network Density, RND	The density (or total length) of the road network per unit area reflects route selection and transportation connectivity.	OSM road network data
8	Accessibility of Transportation Station, ATS2	The difficulty for people to reach the nearest public transportation station reflects the location accessibility of street space.	OSM road network data
9	Diversity of Commercial Facilities, DCF	Use Shannon's index to calculate the mixing degree of various POIs to reflect the diversity of commercial facilities.	POI data
10	Density of Leisure and Shopping, DLS	The density of leisure shopping POIs within the 100 m buffer zone of the road reflects the convenience of leisure shopping.	POI data
11	Accessibility of Life Services, ALS	The density of life service POIs within the 100 m buffer zone of the road reflects the convenience of life services.	POI data
12	Diversity of Diverse Functions, DDF	Use Shannon's diversity index (SHDI) to calculate the mixing degree of various POIs to reflect the diversity of facilities.	POI data
13	Street Enclosure, SE	The average proportion of buildings and column elements in street view images within street units reflects the degree of street space congestion.	Semantic segmentation
14	Vehicle Traffic Index, VTI	The average proportion of motor vehicles and motor vehicle lane elements in street images within street units reflects the vehicle space.	Semantic segmentation
15	Density of Cultural and Educational, DCE	The density of cultural and educational facilities POI within the 100 m buffer zone of the road, and the convenience of counter-cultural education.	POI data
16	Medical Facilities Density, MFD	The density of medical facility POIs within the 100 m buffer zone of the road and the convenience of counter-cultural medical care.	POI data

3.5. Calculation of Coefficient of Variation

The coefficient of variation (CV) is a relative statistical measure that quantifies the degree of variation in data. The CV eliminates the impact of differing units or average values when comparing the variability of two or more sets of data. It is utilized to assess the variability among samples with different means and is also employed in the calculation of weights. The formula for calculation is as follows:

$$CV(X) = \frac{\sqrt{\mathrm{Var}(X)}}{\mathrm{E}(X)} = \frac{\sigma(X)}{E(X)} = \frac{SD}{Mean} * 100\% \quad (1)$$

3.6. Principal Component Analysis (PCA)

Historically, researchers have utilized a spectrum of indicators to gauge urban spatial quality. In an effort to identify the predominant factors shaping the quality of street spaces, this study adopts principal component analysis (PCA) to scrutinize the indicators of street spatial quality on the Macau Peninsula. PCA, a statistical technique grounded in dimensionality reduction, enables the transformation of a multitude of variables into a concise set of orthogonal principal components. These components encapsulate the maximum variance within the data while maintaining minimal loss of information and ensuring the components are mutually uncorrelated [82,83]. The procedure commences with the standardization of the raw data, followed by the construction of a correlation matrix among the variables. Subsequently, eigenvectors are utilized to derive new composite variables, referred to as principal components. The process involves calculating the contribution rate of each eigenvalue and its cumulative effect, culminating in the determination of a composite score.

In the context of this study, the high-dimensional data of street quality, comprising 16 variables, is condensed into a smaller set of principal components through PCA. Recognizing that a solitary principal component is inadequate to encapsulate the original p variables, the study endeavors to identify secondary, tertiary, and even quaternary components. Each principal component is meticulously determined to ensure its independence from the others, thereby providing a comprehensive and nuanced representation of the original dataset. The method for ascertaining these components is delineated as follows:

Let z_i represent the i principal component for, i = 1, 2, . . ., p, and the formulation can be posited as follows:

$$\begin{cases} Z_1 = C_{11}X_1 + C_{12}X_2 + \cdots + C_{1p}X_p \\ Z_2 = C_{21}X_1 + C_{22}X_2 + \cdots + C_{2p}X_p \\ \cdots \\ Z_p = C_{p1}X_1 + C_{p2}X_2 + \cdots + C_{pp}X_p \end{cases} \quad (2)$$

where, for each i, there are

$$C_{i1}^2 + C_{i2}^2 + \cdots + C_{ip}^2 = 1 \quad (3)$$

First, the raw data are normalized to eliminate the effect of the dimension. Assuming that there are m indicator variables for the principal component analysis: x_1, x_2, . . . x_m, where there are n evaluation objects and the value of the j indicator of the i evaluation object is x_{ij} , the value of each indicator is transformed into a standardized indicator $\overline{x}_{ij}$,

$$\overline{x}_{ij} = \frac{x_{ij} - \overline{x}_j}{s_j}, (i = 1, 2, \ldots, n; j = 1, 2, \ldots, m) \quad (4)$$

where

$$\overline{x} = \frac{1}{n}\sum_{i=1}^{n} x_{ij}, sj = \frac{1}{n-1}\sum_{i=1}^{1} (x_{ij} - \overline{x}_j)^2, (j = 1, 2, \ldots, m) \quad (5)$$

That is, $\overline{x}_j$, s_j are the sample mean and sample standard deviation of the j indicator.

Correspondingly, call $\overline{x}_i = \frac{x_i - \overline{x}_i}{s_j}, (i = 1, 2, \ldots, m)$ as the standardized indicator variables.

Create a matrix of correlation coefficients between the variables R. The correlation coefficient matrix is as follows:

$$R = \left(r_{ij}\right)_{m \times m} \tag{6}$$

$$r_{ij} = \frac{\sum_{k=1}^{m} \overline{x}_{ki} \cdot \overline{x}_{kj}}{n-1}, (i, j = 1, 2, \ldots, m) \tag{7}$$

where $r_{ii} = 1, r_{ij} = r_{ji}, r_{ij}$ is the correlation coefficient between the i indicator and the j indicator.

Calculate the eigenvalues of the correlation coefficient matrix R $\lambda_1 \geq \lambda_2 \geq \Delta \geq \lambda_m \geq 0$ and the corresponding eigenvectors $u_1, u_2, \ldots, u_m$, where $u_j, = (u_{1j}, u_{2j}, \ldots, u_{nj})^{\mathrm{T}}$, are composed of the eigenvectors to form m new indicator variables.

$$\begin{cases} y_1 = u_{11}\overline{x}_1 + u_{21}\overline{x}_2 + \cdots + u_{n1}\overline{x}_p \\ y_2 = u_{12}\overline{x}_1 + u_{22}\overline{x}_2 + \cdots + u_{n2}\overline{x}_p \\ \cdots \\ y_m = u_{1m}\overline{x}_1 + u_{2m}\overline{x}_2 + \cdots + u_{nm}\overline{x}_p \end{cases} \tag{8}$$

where y_1 is the first principal component, y_2 is the second principal component $\ldots$, y_m is the m principal component.

Calculate the information contribution and cumulative contribution of the eigenvalues $\lambda_1 = (j = 1, 2, \ldots, m)$. Call

$$b_j = \frac{\lambda_j}{\sum_{k=1}^{m} \lambda_k} (j = 1, 2, \ldots m) \tag{9}$$

is the information contribution of the main component y_j.

$$a_p = \frac{\sum_{k=1}^{p} \lambda_k}{\sum_{k=1}^{m} \lambda_k} \tag{10}$$

is the cumulative contribution of the principal components $y_1, y_2, \ldots, y_p$. When a_p is close to 1 ($a_r = 0.85, 0.90, 0.95$), the first p principal components are selected to replace the original m indicator variables, so that the p principal components can be analyzed comprehensively.

Calculate the composite score as follows:

$$Z = \sum_{j=1}^{p} b_j y_j \tag{11}$$

where b_j is the information contribution of the j principal component.

4. Results

4.1. Descriptive Statistical Analysis of Street Spatial Quality Indicators

This study employed the computational methods detailed in Table 1 to evaluate the street space quality, yielding numerical values for 16 indicators, including the GVI, GCI, SKI, CRI, AP, ATS, RND, ATS2, DCF, DLS, ALS, DDF, SE, VTI, and DCE, among others. Descriptive statistical analysis, including the mean, median, and standard deviation, was performed on these indicators, with the results presented in Table 2.

The coefficient of variation (CV) for the street space quality indicators was calculated using Equation (1) to assess the variability of each metric. The CV, which normalizes the standard deviation by the mean, enables the comparison of the variability between different indicator datasets, thus evaluating the uniformity and stability of the street quality indicators. CV values are commonly classified as indicating low variability (CV $\leq$ 10%), moderate variability (10% < CV $\leq$ 100%), and high variability (CV > 100%) [84,85].

Table 2. Descriptive statistics of the spatial quality of streets.

	GVI	GCI	SKI	CRI	AP	ATS	ATS2	RND	DCF	DLS	ALS	DDF	SE	VTI	DCE	MFD
Maximum	43.50	12.12	67.00	0.78	14.08	57.00	901.99	20,218.8	1.58	214.00	74.00	2.25	65.89	24.42	33.01	112.01
Minimum	0.00	0.00	0.00	0.00	0.00	0.00	0.07	189.98	0.05	0.00	0.00	0.11	0.00	0.00	0.01	0.01
Average	8.16	12.07	31.45	0.69	4.72	4.64	90.17	11,684.2	0.85	20.59	6.70	1.47	31.83	15.45	2.86	9.18
Median	7.11	12.12	29.26	0.70	4.77	4.00	74.90	11,634.6	0.81	11.00	4.00	1.51	31.79	16.53	2.01	4.01
Standard Error of Mean	0.07	0.01	0.13	0.00	0.02	0.05	0.87	45.80	0.00	0.31	0.10	0.00	0.20	0.05	0.04	0.15
Standard Error	6.11	0.74	10.81	0.07	1.94	4.36	70.90	3739.33	0.30	25.08	7.87	0.35	16.20	3.99	3.44	12.29
Coefficient of Variation%	74.87	6.14	34.36	9.96	41.17	94.01	78.63	32	34.91	121.81	117.51	23.84	50.89	25.86	120.29	133.9

As per Table 2, the green coverage index (GCI) exhibits the lowest variability, with a CV of 6.14%, denoting minimal fluctuation in this indicator. The color richness index (CRI) follows with a CV of 9.96%, also indicating low variability. In contrast, the density of leisure and shopping (DLS), accessibility of life services (ALS), density of cultural and educational (DCE), and medical facilities density (MFD) present higher variability, with CV values surpassing 100%. The elevated CV values for these indicators suggest a lower correlation between sampling points within the area.

Notably, Table 2 also presents the median values for each indicator, offering a robust estimate of the central tendency for street space quality data that may not follow a normal distribution. The median is impervious to the sample size or imbalances in the variability, thereby providing a more precise reflection of the data's central tendency.

4.2. Correlation Analysis of Street Spatial Quality Indicators

In this research, a correlation matrix was established to assess the relationships between 16 indicators of street space quality using the Pearson correlation coefficient. These indicators include the green view index (GVI), green coverage index (GCI), sky view index (SVI), color richness index (CRI), accessibility of pavement (AP), accessibility of transportation services (ATS), road network density (RND), accessibility of transportation station (ATS2), diversity of commercial facilities (DCF), density of leisure and shopping (DLS), accessibility of life services (ALS), diversity of diverse functions (DDF), street enclosure (SE), vehicle traffic index (VTI), density of cultural and educational (DCE), and medical facilities density (MFD). The analysis is illustrated in Figure 5.

Significant positive correlations were identified between the GVI and the indices of SVI, CRI, and VTI ($p < 0.05$; $p < 0.01$). In contrast, the GVI showed significant negative correlations with the AP, ATS, DLS, ALS, SE, DCE, and MFD ($p < 0.05$; $p < 0.01$; $p < 0.001$). A strong positive correlation was observed between the GCI and CRI ($p < 0.001$). The SVI also correlated positively with the CRI and VTI ($p < 0.05$; $p < 0.001$), and negatively with the AP, ATS, RND, DLS, ALS, SE, DCE, and MFD ($p < 0.001$). The CRI had strong positive associations with the GVI, GCI, and VTI ($p < 0.01$; $p < 0.001$), and weak negative associations with the DLS, ALS, SE, and MFD ($p < 0.05$). The AP was positively related to the DLS, ALS, SE, DCE, and MFD ($p < 0.001$), and negatively related to the VTI ($p < 0.001$). The ATS showed positive correlations with the DLS, ALS, SE, DCE, and MFD ($p < 0.001$), and a negative correlation with the VTI ($p < 0.05$). The DLS was positively correlated with the ALS, SE, DCE, and MFD ($p < 0.001$), and negatively correlated with the VTI ($p < 0.001$). The ALS demonstrated positive correlations with the SE, DCE, and MFD ($p < 0.001$), and a negative correlation with the VTI ($p < 0.01$). The SE was positively associated with the DCE and MFD ($p < 0.001$), and negatively associated with the VTI ($p < 0.001$). Lastly, the VTI showed a negative correlation with the DCE and MFD ($p < 0.01$), while the DCE was positively correlated with the MFD ($p < 0.001$).

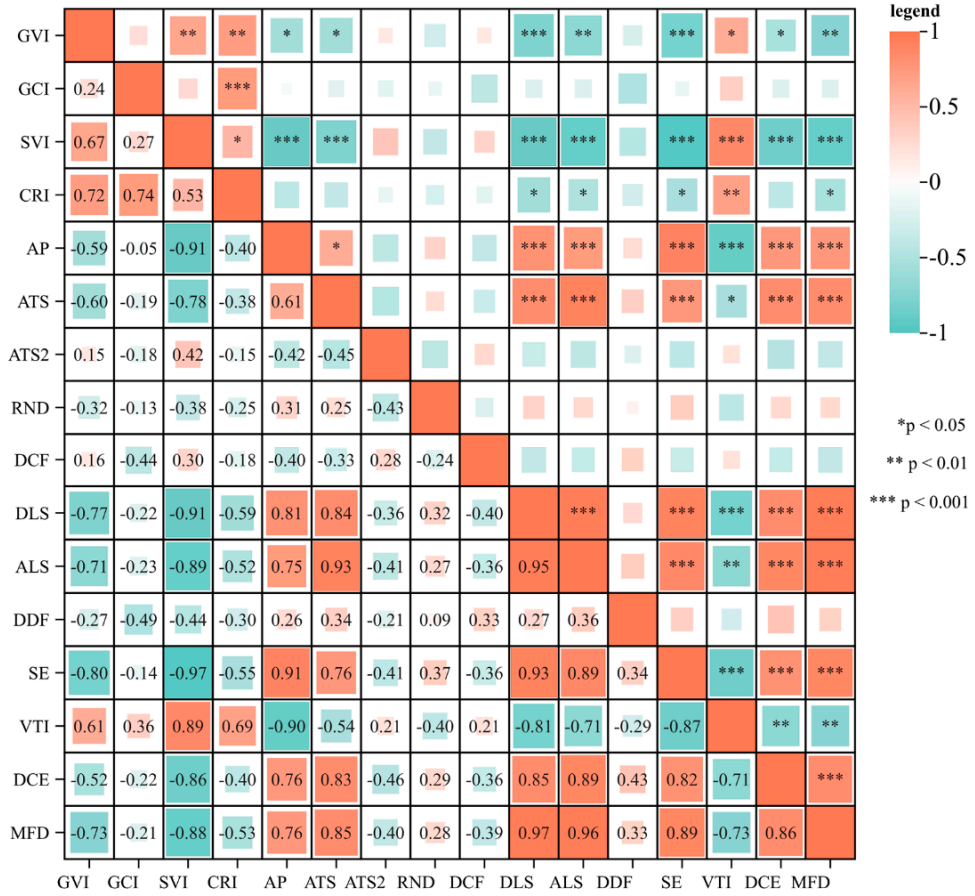


Figure 5. Correlation analysis of the street spatial quality indicators.

4.3. Evaluation of Spatial Quality of Streets Based on Principal Component Analysis

Utilizing a series of equations (4 to 10), this study systematically calculated the eigenvalue spectrum and component matrix that account for the total variance of the principal components representing street space quality, as detailed in Table 3. By selecting principal components with eigenvalues exceeding one, the dimensionality of the data, originally consisting of 16 indicators, was reduced to a more manageable five-dimensional dataset (principal components 1 through 5). These principal components are independent of each other and enhance the representation of the data's inherent structure.

The first principal component (PC1) is characterized by an eigenvalue of 5.218, the second (PC2) by 2.129, the third (PC3) by 1.555, the fourth (PC4) by 1.256, and the fifth (PC5) by 1.087. PC1 predominates in its influence over the dataset, explaining a larger portion of the variance, with each subsequent component contributing less variance than the previous one. The cumulative variance explained by the first five principal components is 32.613%, 45.918%, 55.638%, 63.487%, and 70.280%, respectively.

A cumulative variance contribution rate above 60% is generally accepted as indicative of a sufficient representation of the dataset's characteristics. In this research, the selected principal components collectively exceed a 70% contribution rate, implying that the derived components are not only representative of the original data but also convey a high degree of information fidelity. This finding supports the use of these five principal components as integrated variables for the assessment of street space quality on the Macau Peninsula, ensuring a high level of rationality and accuracy in the evaluation.

The individual variance contribution rates for each principal component are 32.613% for PC1, 13.305% for PC2, 9.720% for PC3, 7.849% for PC4, and 6.793% for PC5. These rates are pivotal for assessing the relative importance of each component within the principal component analysis framework.

Table 3. Loadings matrix, eigenvalues, and variance contributions of the street spatial quality principal components.

Indicators	Components				
	1	2	3	4	5
SE	0.863	−0.105	−0.222	0.032	0.082
DLS	0.826	0.065	0.035	−0.264	0.031
ALS	0.809	0.250	0.255	−0.215	−0.028
SVI	−0.799	0.163	0.124	−0.289	−0.060
MFD	0.769	0.183	0.159	−0.252	−0.004
AP	0.655	0.002	−0.379	0.344	0.318
DCE	0.649	0.309	0.206	0.144	0.046
ATS	0.611	0.362	0.321	−0.182	−0.145
VTI	−0.548	0.543	0.316	−0.295	−0.180
CRI	−0.231	0.865	−0.165	0.218	0.099
GCI	−0.016	0.697	−0.398	−0.120	0.201
DCF	−0.132	−0.149	0.629	0.308	0.132
DDF	0.255	0.095	0.592	0.481	0.022
GVI	−0.415	0.413	0.041	0.435	0.197
RND	0.209	0.026	−0.132	0.235	−0.657
ATS2	−0.179	−0.183	0.246	−0.315	0.617
Eigenvalue	5.218	2.129	1.555	1.256	1.087
Variance percentage %	32.613	13.305	9.720	7.849	6.793
Accumulated contribution rate %	32.613	45.918	55.638	63.487	70.280

Based on the eigenvalues of the total variance interpretation table in Table 3 and the component matrix table, the eigenvectors of each principal component were calculated and are shown in Table 4.

Table 4. Matrix of coefficients of the principal component scores for the spatial quality of streets.

Indicators	Components				
	1	2	3	4	5
SE	0.378	−0.072	−0.178	0.029	0.079
DLS	0.362	0.045	0.028	−0.236	0.030
ALS	0.354	0.171	0.205	−0.192	−0.027
SVI	−0.350	0.112	0.099	−0.258	−0.058
MFD	0.337	0.125	0.128	−0.225	−0.004
AP	0.287	0.001	−0.304	0.307	0.305
DCE	0.284	0.211	0.165	0.129	0.045
ATS	0.268	0.248	0.257	−0.162	−0.139
VTI	−0.240	0.372	0.253	−0.263	−0.172
CRI	−0.101	0.593	−0.132	0.195	0.095
GCI	−0.007	0.478	−0.319	−0.107	0.193
DCF	−0.058	−0.102	0.504	0.275	0.127
DDF	0.112	0.065	0.475	0.429	0.022
GVI	−0.182	0.283	0.033	0.388	0.189
RND	0.091	0.018	−0.106	0.210	−0.630
ATS2	−0.078	−0.125	0.197	−0.281	0.591

This resulted in a linear expression for the five principal components with the original 16 indicators.

$$y_1 = 0.378SE + 0.362DLS + 0.354ALS - 0.35SKI + 0.337MFD + 0.287AP + 0.284DCE + 0.268ATS - 0.24VTI - 0.101CRI - 0.007GCI - 0.058DCF + 0.112DDF - 0.182GVI + 0.091RND - 0.078ATS2 \quad (12)$$

$$y_2 = 0.072SE + 0.045DLS + 0.171ALS + 0.112SKI + 0.125MFD + 0.001AP + 0.211DCE + 0.248ATS + 0.372VTI + 0.593CRI + 0.478GCI - 0.102DCF + 0.065DDF + 0.283GVI + 0.018RND - 0.125ATS2 \quad (13)$$

$$y_3 = 0.178SE + 0.028DLS + 0.205ALS + 0.099SKI + 0.128MFD - 0.304AP + 0.165DCE + 0.257ATS + 0.253VTI - 0.132CRI - 0.319GCI + 0.504DCF + 0.475DDF + 0.033GVI - 0.106RND + 0.197ATS2 \quad (14)$$

$$y_4 = -0.029SE - 0.236DLS - 0.192ALS - 0.258SKI - 0.225MFD + 0.307AP + 0.129DCE - 0.162ATS - 0.263VTI + 0.195CRI - 0.107GCI + 0.275DCF + 0.429DDF + 0.388GVI + 0.21RND - 0.281ATS2 \quad (15)$$

$$y_5 = 0.079SE + 0.030DLS - 0.027ALS - 0.058SKI - 0.004MFD + 0.305AP + 0.045DCE - 0.139ATS - 0.172VTI + 0.095CRI + 0.193GCI + 0.127DCF + 0.022DDF + 0.189GVI - 0.63RND + 0.591ATS2 \quad (16)$$

Using the standardized data of the 16 urban street spatial quality indicators brought into Equations (12)–(16), the composite scores obtained for all the streets on the five principal components could be derived. A function expression was then derived from Equation (11):

$$Z = 0.32613y1 + 0.13305y2 + 0.0972y3 + 0.07849y4 + 0.06793y5 \quad (17)$$

The comprehensive scores of the different indicators of street spatial quality were calculated according to the above comprehensive evaluation model, and the results are shown in Figure 6, from which it can be seen that, in terms of the distribution of the comprehensive scores of the street spatial quality on the Macau Peninsula, the scores of the collection points were mainly concentrated between −0.88 and 0.92, with the greatest number of collection points with a distribution of scores ranging from −0.58 to −0.43. In addition, to obtain a deeper understanding of the distribution of the composite scores, this study presents the ten collection points with the highest composite scores for the street pictures and indicators of street quality (see Figure 7).

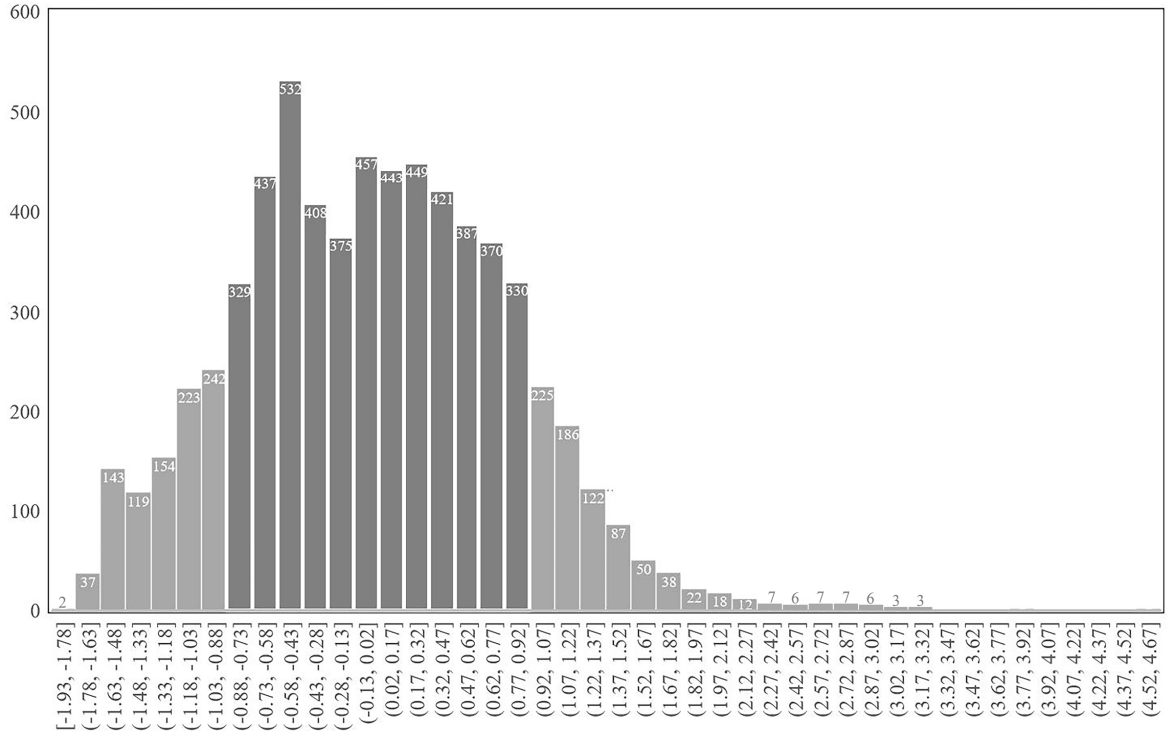


Figure 6. Distribution of the street spatial quality composite scores.

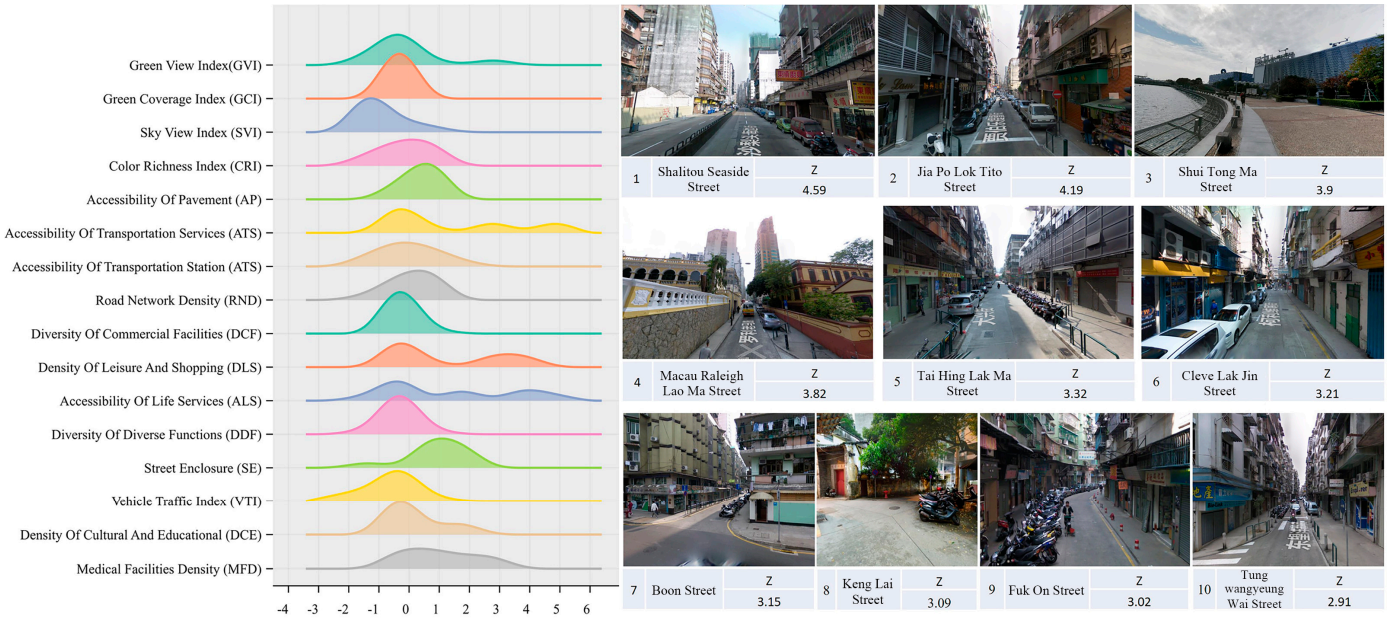


Figure 7. Map of the ten street collection points and peaks with the highest combined street spatial quality scores (street view from Google Maps).

4.4. Cluster Analysis of Spatial Quality Indicators for Streets

The analysis presented in this study reveals the existence of intercorrelations among certain spatial quality indicators on the Macau Peninsula. Given the complexity of categorizing multiple indicators, a classification method based on a single indicator is insufficient for a comprehensive description. Therefore, a holistic approach that considers multiple factors is required. Cluster analysis, a method that classifies objects or indicators based on various characteristics, aggregates those with the highest similarity into progressively larger groups. This process ultimately forms multiple categories, completing the clustering process. This study further applies cluster analysis to the indicators of street space quality, with the results illustrated in Figure 8.

The cluster analysis diagram discerns three distinct clusters, each comprising street space quality indicators with analogous attributes. The first cluster encompasses five indicators: diversity of diverse functions (DDF), density of cultural and educational (DCE), diversity of commercial facilities (DCF), road network density (RND), color richness index (CRI), and green coverage index (GCI). This cluster primarily consolidates urban functional facilities and landscape indicators, aligning with the results of the principal component analysis shown in Table 3, where these indicators are categorized as having lower scores and contribution rates within the first principal component.

The second cluster comprises four indicators: vehicle traffic index (VTI), sky view index (SVI), green view index (GVI), and accessibility of transportation station (ATS2). This cluster mainly groups urban traffic functional facilities and landscape indicators.

The third cluster includes five indicators: density of cultural and educational (DCE), accessibility of transportation services (ATS), medical facilities density (MFD), density of leisure and shopping (DLS), and accessibility of life services (ALS). This cluster predominantly aggregates urban public service facility indicators, which correspond with the results of the principal component analysis shown in Table 3, positioning these indicators at a mid-to-high level in terms of the score and contribution rate within the first principal component.

The fourth cluster contains two indicators: street enclosure (SE) and accessibility of pavement (AP). This cluster focuses on the urban street landscape interface conditions, correlating with the results of the principal component analysis shown in Table 3, where these indicators rank high in the score and contribution rate within the first principal component.

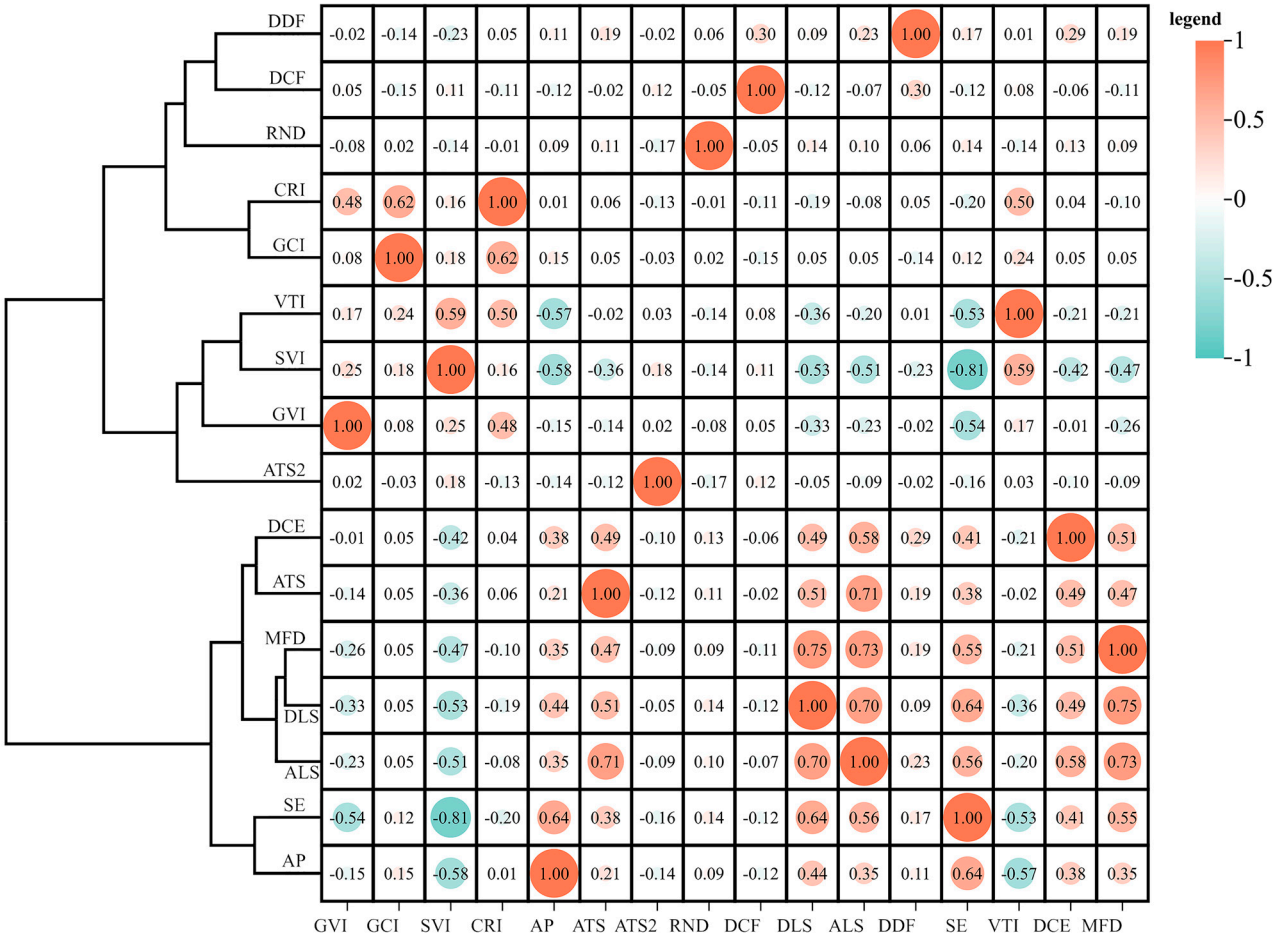


Figure 8. Spectra of the cluster analysis of the spatial quality indicators of streets.

5. Discussion

5.1. Indicators' Coefficient of Variation

This study on the street quality of the Macau Peninsula indicators has identified a low coefficient of variation (CV) for the green coverage index (GCI), signifying limited variability. This low variability is a consequence of the region's advanced urbanization, which has allocated substantial land for construction and infrastructure at the expense of green spaces. The peninsula's role as a commercial and tourism nexus further exacerbates the pressure on local vegetation, leading to a diminished GCI. The greening rate indicator's medium CV corroborates scholarly discussions on the distinctions between green coverage and the greening rate [3,18]. The green coverage rate refers to the proportion of urban surfaces covered by vegetation, such as lawns, trees, and gardens, whereas the greening rate measures the ratio of green space to the total urban area. The Macau Peninsula's vegetation coverage is deemed inadequate, aligning with Ye [76], who noted the inequitable distribution of urban green spaces.

The color richness index (CRI) similarly displays a low CV, attributable to the geographical constraints on the natural color diversity and the influence of Macau's historical and cultural heritage [1,77]. The region's colonial past has left a mark on its architectural and urban-planning choices, favoring a more conservative color scheme. The impact of commercialization on the city's aesthetic, catering to a broad audience, has also stifled uniqueness and innovation, culminating in a lower CRI.

The serviceability indicators of street space, including the density of leisure and shopping (DLS), accessibility of life services (ALS), density of cultural and educational facilities (DCE), and medical facilities density (MFD), exhibit higher variability, with CVs

surpassing 100%. Despite their uneven distribution, these metrics remain within acceptable limits. The accessibility of transportation services (ATS) and transportation stations (ATS2) report CVs approaching 100%. The green view index (GVI) peaks at 74.87% within the 10% to 100% CV range, underscoring significant variance in the street space quality and indicating low inter-point correlation. Collectively, the CVs of the studied indicators fall within acceptable parameters.

5.2. Indicators' Correlation Coefficient

The correlation analysis of the pivotal indicators in this study has uncovered a robust positive association between the green view index (GVI) and other indices, namely the sky view index (SVI), color richness index (CRI), and view transparency index (VTI). This correlation underscores the beneficial connection between urban green spaces and the expansiveness of visual landscapes. Conversely, a significant negative correlation between the GVI and a suite of public service facility indicators, including the accessibility of pavement (AP), accessibility of transportation services (ATS), density of leisure and shopping (DLS), accessibility of life services (ALS), street enclosure (SE), density of cultural and educational facilities (DCE), and medical facilities density (MFD), indicates a tension in land utilization between these services and green spaces within the urban fabric of Macau.

The green coverage index (GCI) correlates notably with the CRI, suggesting that the presence of greenery enhances the diversity of urban colors, yet it does not significantly relate to the other indices. This may be due to the limited spatial extent of the GCI in dense urban contexts and its optimal visibility from an aerial perspective, which contrasts with the ground-level vantage point of this study's data collection.

A strong positive correlation between the SVI and both the CRI and VTI indicates that areas offering broader sky vistas also boast a richer color palette, which could amplify the streets' aesthetic and social dynamics. In contrast, a strong negative correlation between the SVI and the living service facility indicators is observed, potentially a consequence of Macau's high-density urban pattern, spatial constraints, and population density, leading to an increased commercial building concentration and high building enclosure that constricts the sky view.

The CRI's strong correlation with both the GVI and GCI further illustrates the contribution of natural elements to the urban color palette. However, the influence of the living service facility indicators on the color richness appears to be less pronounced. A robust positive correlation between the accessibility of pavement (AP), accessibility of transportation services (ATS), and other living service facility indicators suggests excellent accessibility to these amenities. Yet, a strong negative correlation between the AP, ATS, and the vehicle traffic index (VTI) implies that high vehicle traffic may detract from pedestrian accessibility.

The intra-category correlations among the living service facility indicators reveal a high concentration of these facilities in Macau's dense urban environment. The high enclosure density around educational and medical institutions leads to traffic congestion and often results in one-way traffic regulations, correlating negatively with vehicular accessibility. Meanwhile, weaker correlations are observed for the GCI, ATS2, road network density (RND), DCE, and population density (DDF) with the other indices, likely due to the ground-level perspective of data collection and their reduced significance within the service quality context. This finding is consistent with Zhang [6], who discovered a tight linkage between urban aesthetics and the configuration of street networks.

5.3. Street Quality Composite Scores

This research utilizes principal component analysis (PCA) as a method of dimensionality reduction, replacing the original 16 indicators with a concise set of composite indicators that encapsulate the majority of the information. This approach effectively filters out the less significant variables while preserving those of substantial importance. Figure 6 illustrates that the comprehensive scores for street space quality on the Macau Peninsula span from negative to positive values, predominantly ranging between −0.88 and 0.92.

This range indicates that the evaluation model can discern the spectrum of street space quality from lower to higher quality areas. A clustering of scores between −0.58 and −0.43 is observed, which may suggest commonalities in the issues faced by streets within this scoring bracket. Figure 7 provides further insight, showing that the top ten street space quality collection points with the highest comprehensive scores are characterized by elevated values for indicators such as the color richness index (CRI), accessibility of pavement (AP), road network density (RND), accessibility of transportation station (ATS), density of leisure and shopping (DLS), street enclosure (SE), density of cultural and educational (DCE) facilities, and medical facilities density (MFD), with particular emphasis on the AP and SE. To provide a clear visual representation of the principal components (y1–y5) and the composite score (z) of street spatial quality, the scores of these six dimensions were mapped using ArcGIS, with a particular focus on several representative streets in the Macau Peninsula, as illustrated in Figure 9. The values for the first principal component (y1) range from 0.65 to 3.40; for the second principal component (y2), they range from −2.38 to 1.13; for the third principal component (y3), the range is −0.06 to 2.01; for the fourth principal component (y4), the values are between −1.21 and 1.64; and for the fifth principal component (y5), the scores fall between −1.35 and 2.27. The composite score (z) is visualized with a range from −0.84 to 1.34, which is found to be largely consistent with the bar chart presented in Figure 6.

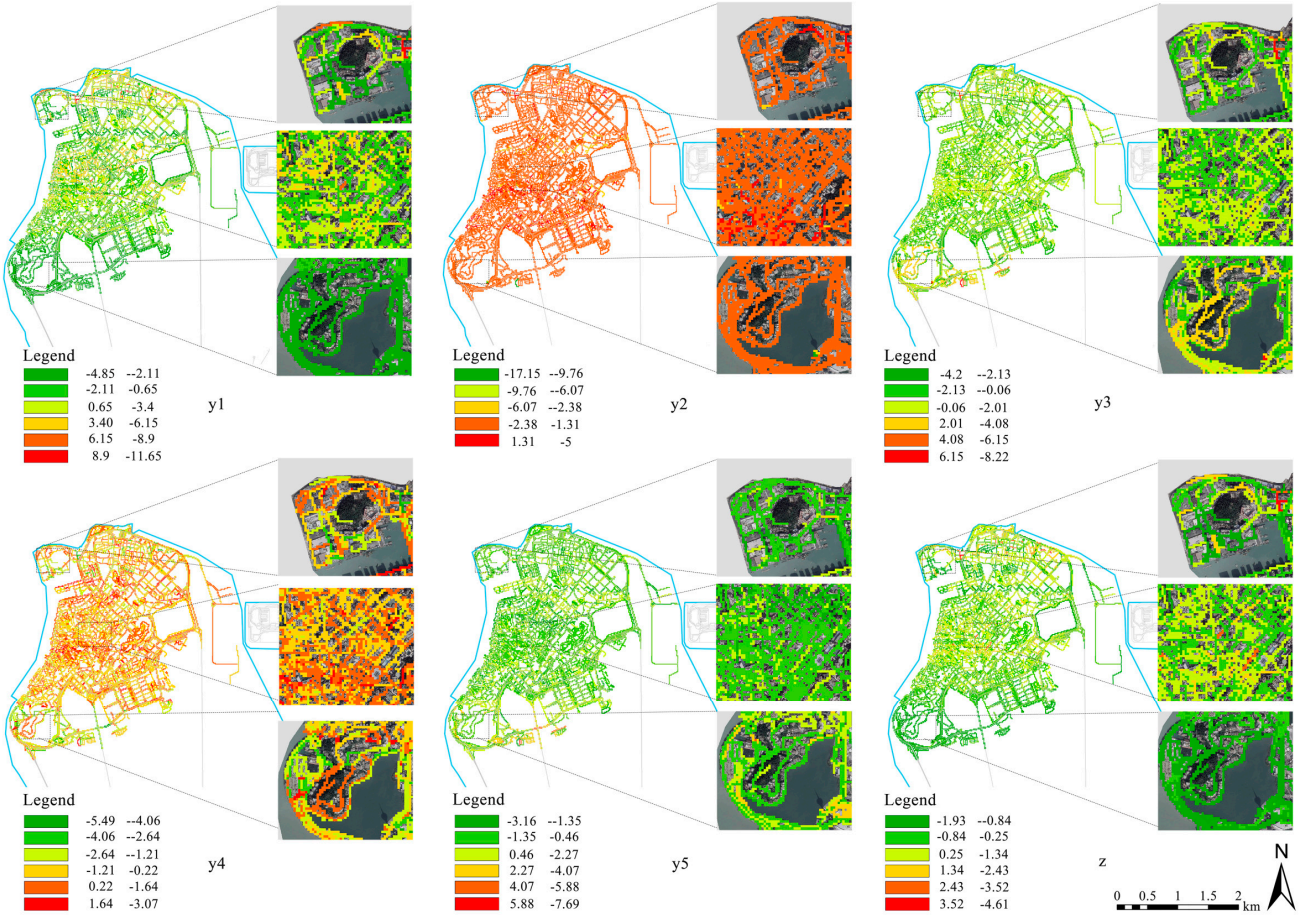


Figure 9. The five principal component scores and total score of street spatial quality, where the value of the first principal component (**y1**) ranges from 0.65 to 3.40; The value of the second principal component (**y2**) ranges from −2.38 to 1.13; The value of the third principal component (**y3**) ranges from −0.06 to 2.01; The values of the fourth principal component (**y4**) are −1.21 and 1.64; The values of the fifth principal component (**y5**) are −1.35 and 2.27; The comprehensive score (**z**) ranges from −0.84 to 1.34.

Analysis of street view imagery reveals the Macau Peninsula's dense road network, where a mere 9.3 square kilometers encompasses 2384 urban roads of varying hierarchy, contributing to a high level of street enclosure [76]. Despite the narrowness of these roads and the prevalence of one-way traffic on secondary routes, they still offer ample pedestrian access and efficient transportation services. The urban architecture is noted for its colorful palette, further enhanced by the dynamic leisure and shopping amenities and their associated signage [32,33]. The collection points with the highest street space quality scores, as gleaned from Google Street View, predominantly consist of secondary urban roads with high enclosure, narrow dimensions, and one-way traffic, except for the first-ranked main road, Rua da Ribeira do Patane, and the third-ranked coastal secondary road, Estrada do Reservatório. Notably, the absence of urban green spaces or vegetation in these top-ranked streets contrasts with the outcomes reported by Li [13] and Ye [3].

5.4. Cluster Analysis Results

Cluster analysis offers an exploratory tool for deciphering intricate datasets concerning spatial quality. However, its insights are best complemented by additional quantitative and qualitative research to yield a holistic view. In the context of cluster analysis, the formation of cohesive clusters among certain indicators suggests a robust correlation in shaping the quality of street spaces [75]. This method effectively aggregates research subjects with closely related attributes into distinct categories, delineating clear classification boundaries while preserving the integrity of the data. It is important to recognize that cluster analysis does not ascribe differential importance to indicators; all the clusters are considered of equal significance.

Upon applying cluster analysis to the street space quality indicators of the Macau Peninsula, this study discerned notable interrelations among various indicators. A classification approach reliant on a solitary indicator is inadequate for a comprehensive description of the categories; hence, a multifactorial classification model is warranted. The analysis stratified the indicators into four clusters, each encapsulating indicators with analogous attributes. These clusters, which embody unique amalgams of spatial quality traits, underscore the heterogeneity of the street space quality within the Macau Peninsula.

The findings align well with the principal component analysis scores, substantiating efforts to augment the street space quality on the Macau Peninsula. Cluster analysis, when applied to multiple indicators, facilitates a more precise identification and categorization of diverse aspects of street space quality. It also mirrors how the urban landscape and land-use configurations on the Macau Peninsula could generate varied combinations of spatial quality indicators [1]. For example, commercial zones may exhibit heightened DCF, DLS, and ATS, whereas residential areas may display elevated GVI and GCI, with an optimized integration of micro-scale green spaces [3]. These insights contribute to the discourse on urban planning and design.

6. Conclusions

This research presents a comprehensive analysis of various indicators of street space quality on the Macau Peninsula, revealing their variability and interrelationships, thus providing valuable insights for urban planning and design.

Initially, the green coverage index (GCI) and the color richness index (CRI) demonstrated low variability, indicative of the constraints on green spaces within the highly urbanized Macau Peninsula, influenced by tourism and commercial activities. Although the GCI showed moderate variability, the overall greening level is considered insufficient. The low variability of the CRI can be attributed to the peninsula's environmental color uniformity, conservative historical and cultural color preferences, and the lack of color innovation due to modern commercialization.

Subsequently, serviceability indicators such as the density of leisure and shopping (DLS), accessibility of life services (ALS), density of cultural and educational facilities (DCE), and medical facilities density (MFD) exhibited high variability, with coefficient of

variation (CV) values surpassing 100%, reflecting the uneven distribution of urban street space service facilities. Correlation analysis indicated a strong positive relationship between the green view index (GVI) and the sky view index (SVI), CRI, and view transparency index (VTI), signifying a beneficial connection between urban green spaces and scenic visibility. Conversely, a strong negative correlation was observed between the GVI and the public service facility indicators, highlighting the land-use conflicts between public services and green spaces in dense urban environments. Moreover, a strong positive correlation among the living service facility indicators (e.g., DLS, DCE, MFD) underscores the concentration of these facilities in the Macau Peninsula's high-density urban context.

Employing principal component analysis and cluster analysis, this study further exposed the diversity of street space quality on the Macau Peninsula. The comprehensive scores for street space quality, ranging from −0.88 to 0.92, demonstrate the evaluation model's capability to discern variations in street space quality. Cluster analysis categorized the indicators into four distinct clusters, each representing a unique combination of spatial quality characteristics.

This study primarily employed principal component analysis (PCA) for the dimensionality reduction of multiple street quality indicators. While the key techniques of PCA have yielded anticipated outcomes, several debates persist. For instance, PCA necessitates data standardization to ensure the equitable contribution of each variable to the analysis. However, some researchers contend that improper standardization may lead to misleading conclusions [86]. In this research, we utilized the Z-score standardization method, ensuring all the variables were compared on a uniform scale, thereby mitigating biases arising from differing units of measurement. Secondly, another contentious issue is the interpretability of the principal components extracted by PCA, which can be challenging to understand, particularly when they represent complex combinations of multiple original variables [87]. Our study enhances the interpretability of the principal components through a detailed rotation method, ensuring each component represents a coherent set of variables. Thirdly, some scholars argue that an overreliance on PCA and other dimensionality reduction techniques might overlook significant individual differences and subtle relationships among variables [82]. By integrating additional statistical methods and qualitative analysis, we endeavored to visualize extensive data, ensuring that the PCA results were not isolated but were combined with other data and theoretical frameworks for a more comprehensive perspective. Fourthly, PCA has certain requirements regarding the sample size and data quality. Small samples or datasets containing noise may lead to inaccurate outcomes [88]. This study utilized a sufficiently large sample size and conducted rigorous data cleaning and quality control to ensure the reliability of the analysis. Fifthly, determining the number of principal components to retain entails a subjective decision-making process, with different choices potentially leading to varying interpretations and conclusions [89]. We selected the number of principal components based on the principle of the cumulative contribution rate and eigenvalues greater than one. Therefore, while PCA analysis has its limitations, this study effectively circumvented the potential issues, providing a robust approach to the dimensionality reduction of street quality indicators.

In conclusion, this study highlights the importance of considering multiple critical factors in urban planning and design to foster coordinated development and enhance urban space quality. The findings suggest that improving the street space quality requires a multifaceted approach, including increasing the green coverage, diversifying the urban colors, and optimizing the distribution of public service facilities. These results align with previous studies conducted in Macau [1,3,77] and offer concrete guidance for urban planning and design, emphasizing the importance of a multi-indicator approach and potential directions for enhancing street space quality on the Macau Peninsula.

This study's limitation lies in its exclusive focus on the built environment within complex, high-density urban areas, neglecting user perceptions. Future research could expand upon the findings of this study by incorporating the GWPCA method proposed by Wu [90] for assessing community visual characteristics and spatial heterogeneity. Moreover,

future studies could explore this by examining user psychological aspects such as the accessibility of green spaces, green space distribution, safety perception, and mental health, particularly in the context of Macau's high-density urban environment. Furthermore, this study is timely in considering the community scale at the micro level, building upon the research findings of Chen [4]. It integrates the "3D" theoretical perspective with urban morphology and people-oriented, environmentally friendly principles to assess and verify the quality and vitality of urban spaces. This approach is essential for formulating effective urban policies and interventions that can enhance community vitality and contribute to the sustainable development of urban areas.

Funding: This research received no external funding.

Data Availability Statement: The data used in this paper mainly came from Open Street Map (https://www.openstreetmap.org/, 19 June 2024), Street View Image (https://map.baidu.com/, 20 April 2024), POI data (https://www.google.com/maps/, 30 May 2024).

Conflicts of Interest: The authors declare no conflict of interest.

References

1. Li, Z.; Quan, S.J.; Yang, P.P.J. Energy performance simulation for planning a low carbon neighborhood urban district: A case study in the city of Macau. *Habitat Int.* **2016**, *53*, 206–214. [CrossRef]
2. Long, Y.; Liu, L. How green are the streets? An analysis for central areas of Chinese cities using Tencent Street View. *PLoS ONE* **2017**, *12*, e0171110. [CrossRef] [PubMed]
3. Ye, Y.; Richards, D.; Lu, Y.; Song, X.; Zhuang, Y.; Zeng, W.; Zhong, T. Measuring daily accessed street greenery: A human-scale approach for informing better urban planning practices. *Landsc. Urban Plan.* **2019**, *191*, 103434. [CrossRef]
4. Chen, J.; Tian, W.; Xu, K.; Pellegrini, P. Testing Small-Scale Vitality Measurement Based on 5D Model Assessment with Multi-Source Data: A Resettlement Community Case in Suzhou. *ISPRS Int. J. Geo-Inf.* **2022**, *11*, 626. [CrossRef]
5. Wang, M.; He, Y.; Meng, H.; Zhang, Y.; Zhu, B.; Mango, J.; Li, X. Assessing street space quality using street view imagery and function-driven method: The case of Xiamen, China. *ISPRS Int. J. Geo-Inf.* **2022**, *11*, 282. [CrossRef]
6. Zhang, F.; Zhang, D.; Liu, Y.; Lin, H. Representing place locales using scene elements. *Comput. Environ. Urban Syst.* **2018**, *71*, 153–164. [CrossRef]
7. Zeng, C.; Song, Y.; He, Q.; Shen, F. Spatially explicit assessment on urban vitality: Case studies in Chicago and Wuhan. *Sustain. Cities Soc.* **2018**, *40*, 296–306. [CrossRef]
8. Garau, C.; Annunziata, A. A method for assessing the vitality potential of urban areas. The case study of the Metropolitan City of Cagliari, Italy. *City Territ. Archit.* **2022**, *9*, 7. [CrossRef]
9. Shi, J.; Miao, W.; Si, H.; Liu, T. Urban vitality evaluation and spatial correlation research: A case study from Shanghai, China. *Land* **2021**, *10*, 1195. [CrossRef]
10. Ye, Y.; Dai, X.L. The possibility of spatial perception and design application under new technologies and new data conditions. *Era Archit.* **2017**, *5*, 6–13.
11. Naik, N.; Philipoom, J.; Raskar, R.; Hidalgo, C. Streetscore-predicting the perceived safety of one million streetscapes. In Proceedings of the IEEE Conference on Computer Vision and Pattern Recognition Workshops, Columbus, OH, USA, 23–28 June 2014; pp. 779–785.
12. Jiang, B.; Deal, B.; Pan, H.; Larsen, L.; Hsieh, C.H.; Chang, C.Y.; Sullivan, W.C. Remotely-sensed imagery vs. eye-level photography: Evaluating associations among measurements of tree cover density. *Landsc. Urban Plan.* **2017**, *157*, 270–281. [CrossRef]
13. Li, X.; Zhang, C.; Li, W.; Ricard, R.; Meng, Q.; Zhang, W. Assessing street-level urban greenery using Google Street View and a modified green view index. *Urban For. Urban Green.* **2015**, *14*, 675–685. [CrossRef]
14. Chen, M.; Cai, Y.; Guo, S.; Sun, R.; Song, Y.; Shen, X. Evaluating implied urban nature vitality in San Francisco: An interdisciplinary approach combining census data, street view images, and social media analysis. *Urban For. Urban Green.* **2024**, *95*, 128289. [CrossRef]
15. Shen, Q.; Zeng, W.; Ye, Y.; Arisona, S.M.; Schubiger, S.; Burkhard, R.; Qu, H. StreetVizor: Visual exploration of human-scale urban forms based on street views. *IEEE Trans. Vis. Comput. Graph* **2017**, *24*, 1004–1013. [CrossRef] [PubMed]
16. Bhatnagar, R. Machine learning and big data processing: A technological perspective and review. In Proceedings of the International Conference on Advanced Machine Learning Technologies and Applications (AMLTA2018), Cairo, Egypt, 22–24 February 2018; pp. 468–478.
17. Biljecki, F.; Ito, K. Street view imagery in urban analytics and GIS: A review. *Landsc. Urban Plan.* **2021**, *215*, 104217. [CrossRef]
18. Yao, Y.; Wang, J.; Hong, Y.; Qian, C.; Guan, Q.; Liang, X.; Zhang, J. Discovering the homogeneous geographic domain of human perceptions from street view images. *Landsc. Urban Plan.* **2021**, *212*, 104125. [CrossRef]

19. Kang, Y.; Zhang, F.; Gao, S.; Lin, H.; Liu, Y. A review of urban physical environment sensing using street view imagery in public health studies. *Ann. GIS* **2020**, *26*, 261–275. [CrossRef]
20. Kim, H.; Hyungki, K.; Yuna, K.; Soonhung, H. Automatic 3D city modeling using a digital map and panoramic images from a mobile mapping system. *Math. Probl. Eng.* **2014**, *2014*, 383270. [CrossRef]
21. Micusik, B.; Kosecka, J. Piecewise planar city 3D modeling from street view panoramic sequences. In Proceedings of the 2009 IEEE Conference on Computer Vision and Pattern Recognition, Miami, FL, USA, 20–25 June 2009.
22. Crandall, D.J.; Backstrom, L.; Huttenlocher, D.; Kleinberg, J. Mapping the world's photos. In Proceedings of the 18th International Conference on World Wide Web, Madrid, Spain, 20–24 April 2009; pp. 761–770.
23. LeCun, Y.; Bengio, Y.; Hinton, G. Deep learning. *Nature* **2015**, *521*, 436–444. [CrossRef] [PubMed]
24. Arietta, S.M.; Efros, A.A.; Ramamoorthi, R.; Agrawala, M. City forensics: Using visual elements to predict non-visual city attributes. *IEEE Trans. Vis. Comput. Graph.* **2014**, *20*, 2624–2633. [CrossRef]
25. Dubey, A.; Naik, N.; Parikh, D.; Raskar, R.; Hidalgo, C.A. Deep learning the city: Quantifying urban perception at a global scale. In Proceedings of the Computer Vision–ECCV 2016: 14th European Conference, Amsterdam, The Netherlands, 11–14 October 2016; pp. 196–212.
26. Liu, L.; Silva, E.A.; Wu, C.; Wang, H. A machine learning-based method for the large-scale evaluation of the qualities of the urban environment. *Comput. Environ. Urban Syst.* **2017**, *65*, 113–125. [CrossRef]
27. Seiferling, I.; Naik, N.; Ratti, C.; Proulx, R. Green streets- quantifying and mapping urban trees with street-level imagery and computer vision. *Landsc. Urban Plan.* **2017**, *165*, 93–101. [CrossRef]
28. Naik, N.; Kominers, S.D.; Raskar, R.; Glaeser, E.L.; Hidalgo, C.A. Computer vision uncovers predictors of physical urban change. *Proc. Natl. Acad. Sci. USA* **2017**, *114*, 7571–7576. [CrossRef] [PubMed]
29. Hyam, R. Automated image sampling and classification can be used to explore perceived naturalness of urban spaces. *PLoS ONE* **2017**, *12*, e0169357. [CrossRef] [PubMed]
30. Xing, Z.; Zhao, S.; Li, K. Evolution Pattern and Spatial Mismatch of Urban Greenspace and Its Impact Mechanism: Evidence from Parkland of Hunan Province. *Land* **2023**, *12*, 2071. [CrossRef]
31. Peihong, W.; Kai, W.; Kerun, L.; Shufang, F. An evaluation model for the recreational carrying capacity of urban aerial trails. *Tour. Manag. Perspect.* **2023**, *48*, 101152. [CrossRef]
32. Li, K.R.; Yang, Y.Q.; Zheng, Z.Q. Research on color harmony of building façades. *Color Res. Appl.* **2020**, *45*, 105–119. [CrossRef]
33. Li, K.R.; Zheng, Z.Q.; Wang, P.H.; Yan, W.J. Research on the colour preference and harmony of the two-colour combination buildings. *Color Res. Appl.* **2022**, *47*, 980–991. [CrossRef]
34. Mirowski, P.; Grimes, M.K.; Malinowski, M.; Hermann, K.M.; Anderson, K.; Teplyashin, D.; Hadsell, R. Learning to navigate in cities without a map. *arXiv* **2018**, arXiv:1804.00168.
35. Garcia-Garcia, A.; Orts-Escolano, S.; Oprea, S.; Villena-Martinez, V.; Martinez-Gonzalez, P.; Garcia-Rodriguez, J. A survey on deep learning techniques for image and video semantic segmentation. *Appl. Soft. Comput.* **2018**, *70*, 41–65. [CrossRef]
36. Dong, Q.; Cai, J.; Chen, S.; He, P.; Chen, X. Spatiotemporal analysis of urban green spatial vitality and the corresponding influencing factors: A case study of Chengdu, China. *Land* **2022**, *11*, 1820. [CrossRef]
37. Helbich, M.; Yao, Y.; Liu, Y.; Zhang, J.; Liu, P.; Wang, R. Using deep learning to examine street view green and blue spaces and their associations with geriatric depression in Beijing, China. *Environ. Int.* **2019**, *126*, 107–117. [CrossRef] [PubMed]
38. Lopez, R.P.; Hynes, H.P. Obesity, physical activity, and the urban environment: Public health research needs. *Environ. Health* **2006**, *5*, 25. [CrossRef] [PubMed]
39. McMichael, A.J. The urban environment and health in a world of increasing globalization: Issues for developing countries. *Bull. World Health Organ.* **2000**, *78*, 1117–1126. [PubMed]
40. Leslie, E.; Cerin, E. Are perceptions of the local environment related to neighbourhood satisfaction and mental health in adults? *Prev. Med.* **2008**, *47*, 273–278. [CrossRef] [PubMed]
41. Sun, G.; Zhao, J.; Webster, C.; Lin, H. New metro system and active travel: A natural experiment. *Environ. Int.* **2020**, *138*, 105605. [CrossRef] [PubMed]
42. Hummel, D. The effects of population and housing density in urban areas on income in the United States. *Local Econ.* **2020**, *35*, 27–47. [CrossRef]
43. Ki, D.; Chen, Z.; Lee, S.; Lieu, S. A novel walkability index using google street view and deep learning. *Sustain. Cities Soc.* **2023**, *99*, 104896. [CrossRef]
44. Cleland, V.J.; Timperio, A.; Crawford, D. Are perceptions of the physical and social environment associated with mothers' walking for leisure and for transport? A longitudinal study. *Prev. Med.* **2008**, *47*, 188–193. [CrossRef]
45. Liu, Z.; Kemperman, A.; Timmermans, H. Correlates of older adults' walking trip duration. *J. Transp. Health* **2020**, *18*, 100889. [CrossRef]
46. Maisel, J.L. Impact of older adults' neighborhood perceptions on walking behavior. *J. Aging Phys. Act.* **2016**, *24*, 247–255. [CrossRef]
47. Ewing, R.; Handy, S. Measuring the unmeasurable: Urban design qualities related to walkability. *J. Urban Des.* **2009**, *14*, 65–84. [CrossRef]
48. Adkins, A.; Dill, J.; Luhr, G.; Neal, M. Unpacking walkability: Testing the influence of urban design features on perceptions of walking environment attractiveness. *J. Urban Des.* **2012**, *17*, 499–510. [CrossRef]

49. Hamim, O.F.; Kancharla, S.R.; Ukkusuri, S.V. Mapping sidewalks on a neighborhood scale from street view images. *Environ. Plan. B Urban Anal. City Sci.* **2024**, *51*, 823–838. [CrossRef]
50. Zuniga-Teran, A.A.; Orr, B.J.; Gimblett, R.H.; Chalfoun, N.V.; Marsh, S.E.; Guertin, D.P.; Going, S.B. Designing healthy communities: Testing the walkability model. *Front. Archit. Res.* **2017**, *6*, 63–73. [CrossRef]
51. Wu, Y.; Liu, Q.; Hang, T.; Yang, Y.; Wang, Y.; Cao, L. Integrating restorative perception into urban street planning: A framework using street view images, deep learning, and space syntax. *Cities* **2024**, *147*, 104791. [CrossRef]
52. Koo, B.W.; Guhathakurta, S.; Botchwey, N.; Hipp, A. Can good microscale pedestrian streetscapes enhance the benefits of macroscale accessible urban form? An automated audit approach using Google street view images. *Landsc. Urban Plan.* **2023**, *237*, 104816. [CrossRef]
53. Yuan, Y.; Wang, R.; Niu, T.; Liu, Y. Using street view images and a geographical detector to understand how street-level built environment is associated with urban poverty: A case study in Guangzhou. *Appl. Geogr.* **2023**, *156*, 102980. [CrossRef]
54. Niu, T.; Chen, Y.; Yuan, Y. Measuring urban poverty using multi-source data and a random forest algorithm: A case study in Guangzhou. *Sustain. Cities Soc.* **2020**, *54*, 102014. [CrossRef]
55. Meng, Y.; Xing, H.; Yuan, Y.; Wong, M.S.; Fan, K. Sensing urban poverty: From the perspective of human perception-based greenery and open-space landscapes. *Comput. Environ. Urban Syst.* **2020**, *84*, 101544. [CrossRef]
56. Goodchild, M.F. Formalizing place in geographic information systems. In *Communities, Neighborhoods, and Health: Expanding the Boundaries of Place*; Springer: New York, NY, USA, 2010.
57. Vich, G.; Magadán, J.D.; Miralles-Guasch, C. The composition of green spaces and levels of physical activity of older people in Barcelona. In *Congreso Internacional Ciudad y Territorio Virtual (CTV)*; UPC: Madrid, Spain, 2019.
58. Middel, A.; Lukasczyk, J.; Zakrzewski, S.; Arnold, M.; Maciejewski, R. Urban form and composition of street canyons: A human-centric big data and deep learning approach. *Landsc. Urban Plan.* **2019**, *183*, 122–132. [CrossRef]
59. Lynch, K. *The Image of the City*; MIT Press: Cambridge, MA, USA, 1960.
60. Ewing, R.; Cervero, R. Travel and the built environment: A meta-analysis. *J. Am. Plan. Assoc.* **2010**, *76*, 265–294. [CrossRef]
61. Kaplan, S.; Nielsen, T.A.S.; Prato, C.G. Walking, cycling and the urban form: A Heckman selection model of active travel mode and distance by young adolescents. *J. Am. Plan. Assoc.* **2016**, *44*, 55–65. [CrossRef]
62. Moran, M.; Plaut, P.; Baron-Epel, O. Do children walk where they bike? Exploring built environment correlates of children's walking and bicycling. *J. Transp. Land Use* **2016**, *9*, 43–65. [CrossRef]
63. Dias, A.F.; Gaya, A.R.; Pizarro, A.N.; Brand, C.; Mendes, T.M.; Mota, J.; Gaya, A.C.A. Perceived and objective measures of neighborhood environment: Association with active commuting to school by socioeconomic status in Brazilian adolescents. *J. Transp. Health* **2019**, *14*, 100612. [CrossRef]
64. Frank, L.; Kerr, J.; Chapman, J.; Sallis, J. Urban form relationships with walk trip frequency and distance among youth. *Am. J. Health Promot.* **2007**, *21*, 305–311. [CrossRef] [PubMed]
65. Panter, J.; Corder, K.; Griffin, S.J.; Jones, A.P.; van Sluijs, E.M. Individual, socio-cultural and environmental predictors of uptake and maintenance of active commuting in children: Longitudinal results from the SPEEDY study. *Int. J. Behav. Nutr. Phys. Act.* **2013**, *10*, 83. [CrossRef] [PubMed]
66. Dalton, M.A.; Longacre, M.R.; Drake, K.M.; Gibson, L.; Adachi-Mejia, A.M.; Swain, K.; Owens, P.M. Built environment predictors of active travel to school among rural adolescents. *Am. J. Prev. Med.* **2011**, *40*, 312–319. [CrossRef] [PubMed]
67. Yang, Y.; Lu, Y.; Yang, L.; Gou, Z.; Zhang, X. Urban greenery, active school transport, and body weight among Hong Kong children. *Travel Behav. Soc.* **2020**, *20*, 104–113. [CrossRef]
68. Fuller, M.; Moore, R. *An Analysis of Jane Jacobs's The Death and Life of Great American Cities*; Macat Library: London, UK, 2017.
69. Jiang, B.; Claramunt, C. Topological analysis of urban street networks. *Environ. Plan B-Urban.* **2004**, *31*, 151–162. [CrossRef]
70. Zhu, D.; Wang, N.; Wu, L.; Liu, Y. Street as a big geo-data assembly and analysis unit in urban studies: A case study using Beijing taxi data. *Appl. Geogr.* **2017**, *86*, 152–164. [CrossRef]
71. Chen, L.C.; Papandreou, G.; Kokkinos, I.; Murphy, K.; Yuille, A.L. Deeplab: Semantic image segmentation with deep convolutional nets, atrous convolution, and fully connected crfs. *IEEE Trans. Pattern Anal. Mach. Intell.* **2017**, *40*, 834–848. [CrossRef] [PubMed]
72. Redmon, J.; Farhadi, A. YOLO9000: Better, faster, stronger. In Proceedings of the IEEE Conference on Computer Vision and Pattern Recognition, Honolulu, HI, USA, 21–26 July 2017; pp. 7263–7271.
73. Shen, J.; Liu, Y. Small and medium-scale street renewal design method based on "quality-vitality" multi-source data. *Landsc. Archit.* **2023**, *9*, 105–113.
74. Li, Y.; Liu, G. Street space quality evaluation based on street view and POI data. *Geospat. Inf.* **2024**, *2*, 64–67.
75. Zhou, H.; He, S.; Cai, Y.; Wang, M.; Su, S. Social inequalities in neighborhood visual walkability: Using street view imagery and deep learning technologies to facilitate healthy city planning. *Sustain. Cities Soc.* **2019**, *50*, 101605. [CrossRef]
76. Ye, C.; Hu, L.; Li, M. Urban green space accessibility changes in a high-density city: A case study of Macau from 2010 to 2015. *J. Transp. Geogr.* **2018**, *66*, 106–115. [CrossRef]
77. Song, Q.; Wang, Z.; Li, J. Residents' behaviors, attitudes, and willingness to pay for recycling e-waste in Macau. *J. Environ. Manag.* **2012**, *106*, 8–16. [CrossRef] [PubMed]
78. Zhou, B.; Zhao, H.; Puig, X.; Fidler, S.; Barriuso, A.; Torralba, A. Scene parsing through ade20k dataset. In Proceedings of the IEEE Conference on Computer Vision and Pattern Recognition, Honolulu, HI, USA, 21–26 July 2017; pp. 633–641.

79. Cheng, B.; Misra, I.; Schwing, A.G.; Kirillov, A.; Girdhar, R. Masked-attention mask transformer for universal image segmentation. In Proceedings of the IEEE/CVF Conference on Computer Vision and Pattern Recognition, Nashville, TN, USA, 20–25 June 2021.
80. Katz, P. *The New Urbanism. Toward an Architecture of Community*; McGraw-Hill: New York, NY, USA, 1994.
81. Montgomery, J. Making a city: Urbanity, vitality and urban design. *J. Urban Des.* **1998**, *3*, 93–116. [CrossRef]
82. Greenacre, M.; Groenen, P.J.; Hastie, T.; d'Enza, A.I.; Markos, A.; Tuzhilina, E. Principal component analysis. *Nat. Rev. Method Prim.* **2022**, *2*, 100. [CrossRef]
83. Kherif, F.; Latypova, A. Principal component analysis. In *Machine Learning*; Academic Press: Cambridge, MA, USA, 2020.
84. Canchola, J.A.; Tang, S.; Hemyari, P.; Paxinos, E.; Marins, E. Correct use of percent coefficient of variation (% CV) formula for log-transformed data. *MOJ Proteom. Bioinform.* **2017**, *6*, 316–317. [CrossRef]
85. Shechtman, O. The coefficient of variation as an index of measurement reliability. In *Methods of Clinical Epidemiology*; Springer: Berlin/Heidelberg, Germany, 2013.
86. Abdi, H.; Williams, L.J. Computational Statistics. In *Wiley Interdisciplinary Reviews: Computational Statistics*; John Wiley & Sons: Hoboken, NJ, USA, 2010.
87. Hair, J.F. *Multivariate Data Analysis*, 7th ed.; Pearson Prentice Hall: Hoboken, NJ, USA, 2009.
88. Sheskin, D.J. *Handbook of Parametric and Nonparametric Statistical Procedures*, 3rd ed.; Chapman and Hall/CRC Press: Boca Raton, FL, USA, 2003.
89. Jolliffe, I.T. Principal component analysis. In *Encyclopedia of Statistics in Behavioral Science*; John Wiley & Sons: Hoboken, NJ, USA, 2005; pp. 1–9.
90. Wu, C.; Peng, N.; Ma, X.; Li, S.; Rao, J. Assessing multiscale visual appearance characteristics of neighbourhoods using geographically weighted principal component analysis in Shenzhen, China. *Comput. Environ. Urban Syst.* **2020**, *84*, 101547. [CrossRef]

Disclaimer/Publisher's Note: The statements, opinions and data contained in all publications are solely those of the individual author(s) and contributor(s) and not of MDPI and/or the editor(s). MDPI and/or the editor(s) disclaim responsibility for any injury to people or property resulting from any ideas, methods, instructions or products referred to in the content.